Fermi National Accelerator Laboratory

FERMILAB-Pub-94/428-A
December 1995

GENERATION OF DENSITY PERTURBATIONS BY PRIMORDIAL MAGNETIC FIELDS

Eun-jin Kim,[1] Angela Olinto,[2] and Robert Rosner[2]

[1] *Department of Physics*
[2] *Department of Astronomy & Astrophysics*
and
Enrico Fermi Institute, The University of Chicago
5640 S. Ellis Ave, Chicago, IL 60637

Abstract

We study the generation and evolution of density perturbations and peculiar velocities due to primordial magnetic fields. We assume that a random magnetic field was present before recombination and follow the field's effect on the baryon fluid starting at recombination. We find that magnetic fields generate growing density perturbations on length scales larger than the magnetic Jeans length. λ_B, and damped oscillations for scales smaller than λ_B. We derive the magnetic Jeans length explicitly by including the back-reaction of the velocity field onto the magnetic field. For small wavenumbers k (large length scales), we find the magnetic field-induced density power spectrum generally scales as k^4, and peaks at $k \sim \lambda_B^{-1}$. Depending on the strength of the magnetic field and the ultraviolet cutoff of its spectrum, structure can be generated on small scales early in the history of the universe. For a present *rms* magnetic field of 10^{-10} Gauss on intergalactic scales, we find that perturbations on galactic scales could have gone non-linear at $z \simeq 6$. Finally, we discuss how primordial magnetic fields affect scenarios of structure formation with non-baryonic dark matter.

1. Introduction

The past decade has seen tremendous growth in our observational picture of the Universe. The Cosmic Background Explorer (Smoot et al. 1992) and other cosmic background experiments have shown that the large-scale clustering seen in galaxy surveys is consistent with a primordial origin for density perturbations. On the largest scales, where density perturbations are linear (i.e., *rms* variations in the density are smaller than the mean), microwave anisotropy observations point toward an approximately Harrison-Zel'dovich spectrum of initial density perturbations ($P(k) \sim \langle|\delta_k|^2\rangle \propto k$; Smoot et al. 1992; Ganga et al. 1993). Such a spectrum arises naturally in inflationary theories as well as in models based on topological defects.

On scales smaller than $\sim 8h^{-1}$ Mpc (where h is the Hubble constant in units of 100 km/sec/Mpc), galaxy clustering is non–linear, and one needs to rely on numerical studies to get insight into the physics of cluster and galaxy formation. Not only do the density perturbations become non–linear, but the complexity of the physics involved escalates as hydrodynamical effects become important. In this paper, we show that an element of this increased complexity that is often neglected, namely magnetic fields, may play a key role in the formation of structure in the non–linear regime.

Of great relevance to understanding the role of magnetic fields in galaxy formation are the recent observations of Faraday rotation associated with high-redshift Lyman-α absorption systems (Wolfe 1988; Wolfe, Lanzetta, & Oren 1991). These observations suggest that dynamically significant magnetic fields ($B \sim \mu$Gauss) were present in condensations at high redshift. Together with observations of strong magnetic fields in clusters (Kronberg 1994), these observations further support the idea that magnetic fields play a dynamical role in the evolution of structure.

The notion that magnetic fields may play an important role in structuring the universe is not new. The most detailed study was done by Wasserman (1978), who assumed the existence of a random magnetic field at recombination and, by treating it as a "source term," showed that it may act as a source for galaxy-scale density fluctuations. These calculations, however, did not take into account the possibility of fluid back-reactions to the Lorentz force. In this sense, Wasserman's calculations were "kinematic," in a manner exactly opposite to that usually encountered in, for example, magnetic dynamo theory (such magnetically–driven "kinematic" calculations were considered earlier by Vainshtein

& Zeldovich 1972). Hence, the temporal evolution of the magnetic fields was entirely due to the Hubble expansion, and a magnetic Jeans length could not be derived.

In order to describe the implications of random magnetic fields present at recombination for structure formation, we consider the coupled evolution of density perturbations, peculiar velocities, *and* magnetic fields. We include the fluid back-reactions to the magnetic forces, and consider how this type of dynamics determines the power spectrum of the resulting velocity field and density fluctuations. Inclusion of the back-reaction onto the magnetic field allows us to derive the magnetic Jeans length for this problem, λ_B. Thus, we present a consistent linear perturbation analysis of the combined magnetic-fluid evolution equations (in the single-fluid approximation), and compute the present density fluctuations and vorticity under the assumption that random magnetic fields existed before recombination. We show that the resulting spectrum for density perturbations has a general form which is insensitive to the magnetic field spectral index; in general, the spectrum of density perturbations is too steep ($P(k) \propto k^4$) to fit the observed spectrum on large scales, while on small scales magnetic fields introduce a peak in the spectrum around either $k \lesssim \lambda_B^{-1}$ or $k \sim k_{\rm max}$, (where $k_{\rm max}$ is the ultraviolet cutoff of the magnetic field spectrum).

The outline of our paper is as follows: We present the basic magnetohydrodynamic equations used in our analysis, discuss plausible initial conditions, and carry out our linearization, in §2. In §3, we consider the compressible mode and compute the resulting power spectrum and amplitude of the generated density fluctuations. In §4, we present the solutions for the incompressible modes. Our results are discussed in §5. For the sake of clarity, we have placed details of our analysis in the Appendices.

2. The Perturbation Analysis

In this section, we review the physical conditions at the time of recombination, discuss the basic equations used in our analysis, and develop our perturbation scheme.

We assume that random magnetic fields were present at the epoch of recombination and that these were formed through pre-recombination processes (e.g, Hogan 1983; Turner & Widrow 1988; Quashnock, Loeb, & Spergel 1989; Vaschaspati 1991; Ratra 1993; Cheng & Olinto 1994). As the universe cooled through recombination, baryons decoupled from the background radiation, and the baryon Jeans length decreased from scales comparable to the Hubble scale (~ 100 Mpc) to ~ 10 kpc in comoving units. (Throughout this paper, we use comoving length scales, setting the scale factor today to unity, $R(t_0) = 1$; physical length scales at any other time can be found by multiplying the comoving scale by $R(t)$.) After recombination, baryons are free to move on scales larger than the Jeans length, and will do so if there are initial perturbations in the density field due to gravitational instabilities. Concurrently, magnetic fields that were frozen into the baryon-photon plasma before recombination will tend to relax into less tangled configurations once the baryons they are coupled to are free to move. Consequently, density perturbations in the baryons can be generated through the Lorentz force even if the density field is initially smooth, and the initial peculiar velocity field vanishes at recombination. To understand the effect of magnetic fields on the origin of density perturbations, we assume that no initial density perturbations or peculiar velocities were present at recombination, so that all subsequent density perturbations or velocities are induced by magnetic fields alone. (We address the more general case of combining initial density perturbations and magnetic field effects in a subsequent paper.)

To follow the evolution of the density, peculiar velocity, and magnetic field after recombination, we write the basic one-fluid magnetohydrodynamic (MHD) equations in comoving coordinates,

$$\rho\left(\partial_t \mathbf{v} + \frac{\dot{R}}{R}\mathbf{v} + \frac{\mathbf{v}\cdot\nabla\mathbf{v}}{R}\right) = -\frac{\nabla p}{R} - \rho\frac{\nabla\psi}{R} + \frac{(\nabla\times\mathbf{B})\times\mathbf{B}}{4\pi R}, \tag{1}$$

$$\partial_t\rho + 3\frac{\dot{R}}{R}\rho + \frac{\nabla\cdot(\rho\mathbf{v})}{R} = 0, \tag{2}$$

$$\frac{\nabla^2\psi}{R^2} = 4\pi G[\rho - \rho_b(t)], \tag{3}$$

$$\nabla\cdot\mathbf{B} = 0, \tag{4}$$

$$\partial_t(R^2\mathbf{B}) = \frac{\nabla\times(\mathbf{v}\times R^2\mathbf{B})}{R} \tag{5}$$

(cf. Wasserman 1978), where ψ is the gravitational potential, R is the scale factor, $\rho_b = \rho_b(t)$ is the uniform background density, and all other symbols have their usual meaning. We have neglected all viscous and diffusive terms because the relevant Reynolds numbers are very large at recombination.

2.1 Initial Conditions

We begin with the basic assumption that all baryonic matter is uniformly distributed at recombination ($t = t_{\rm rec}$), with density $\rho_b(t = t_{\rm rec})$ and we further assume that this matter has zero peculiar velocity. Furthermore, we assume that there is a magnetic field already present, $\mathbf{B}(\mathbf{x}, t = t_{\rm rec}) = \mathbf{B}_{\rm rec}(\mathbf{x})$, presumably created well before recombination: we posit that this magnetic field is randomly oriented on spatial scales smaller than the Hubble radius at recombination *and* has no mean components on the Hubble scale; thus, we assume that

$$\langle \mathbf{B}_{\rm rec}(\mathbf{x}) \rangle = 0 \,,$$

where the angular brackets mean ensemble averaging.

The basic assumption underlying our calcuation is that the above (frozen–in) magnetic field does not significantly perturb the baryonic matter until photons and baryons decouple; once decoupling occurs, the unbalanced Lorentz forces act to disturb the smooth background density, leading to both density perturbations and peculiar velocities of the baryonic fluid (Wasserman 1978). This physical picture suggests the following scheme for decomposing the three flow variables of interest — the fluid density, the fluid velocity, and the magnetic field: we write

$$\begin{aligned} \rho(\mathbf{x}, t) &= \rho_b(t) + \delta\rho(\mathbf{x}, t) \equiv \rho_b(t)[1 + \delta(\mathbf{x}, t)] \,, \\ \mathbf{v}(\mathbf{x}, t) &= \mathbf{v}_b + \mathbf{v}'(\mathbf{x}, t) \,, \\ \mathbf{B}(\mathbf{x}, t) &= \mathbf{B}_b(\mathbf{x}, t) + \mathbf{b}(\mathbf{x}, t) \,. \end{aligned}$$

Here $\mathbf{B}$ is the total field, $\mathbf{B}_b$ is the background random magnetic field, with $\mathbf{B}_b(\mathbf{x}, t_{\rm rec}) = \mathbf{B}_{\rm rec}(\mathbf{x})$, and $\mathbf{b}$ is the difference between the total field and the background; in other words. $\mathbf{B}_b(t)$ is simply the initial random field evolved only by the Hubble flow, while $\mathbf{b}$ is the additional field which results as the Lorentz force perturbs the baryonic fluid, and the fluid reacts back. Similarly, $\mathbf{v}$ is the total velocity, $\mathbf{v}'$ is the perturbation velocity, ρ is the total density, $\delta\rho$ is the density perturbation, and δ is the non–dimensional density perturbation.

With these definitions, we impose a number of constraints. Note that the background flow is assumed to vanish identically,

$$\mathbf{v}_b \equiv 0 \,.$$

We also assume that the perturbed quantities δ, $\mathbf{v}'$, and $\mathbf{b}$ vanish at $t_{\rm rec}$:

$$\delta(\mathbf{x}, t_{\rm rec}) = 0\,,$$
$$\mathbf{v}'(\mathbf{x}, t_{\rm rec}) = 0\,,$$
$$\mathbf{b}(\mathbf{x}, t_{\rm rec}) = 0\,.$$

Since $\mathbf{v}_b = 0$, we shall drop the prime for the sake of notational economy in the following.

2.2 The Perturbation Scheme

The next step is to identify our "small" quantities, which will fix the ordering of the perturbation scheme. In the spirit of a linearized theory, we shall assume that the density perturbations resulting from the Lorentz force are small, i.e., that

$$\delta \ll 1\,.$$

Similarly, we assume that the induced peculiar velocities and magnetic fields are small, e.g., we assume that

$$\frac{v_{\rm rms}\tau}{LR(t_{\rm rec}+\tau)} \ll 1\,,$$

where τ is the characteristic time scale of the flow, $v_{\rm rms}$ is the *rms* flow speed, and $LR(t_{\rm rec}+\tau)$ is the characteristic length scale of the flow at time $t_{\rm rec}+\tau$. Using these scaling relationships, we linearize eqs. (1)–(5), noting that since we are primarily interested in wavelengths larger than the Jeans length, the pressure term may be ignored. Then, upon retaining terms to first order in δ, $\mathbf{v}$, and $\mathbf{b}$, we obtain

$$\partial_t\mathbf{v} + \frac{\dot{R}}{R}\mathbf{v} = -\frac{\nabla\psi}{R} + \frac{[\nabla\times(\mathbf{B}_b+\mathbf{b})]\times\mathbf{B}_b + (\nabla\times\mathbf{B}_b)\times\mathbf{b}}{4\pi R(t)\rho_b(t)}, \tag{6}$$

$$\partial_t\delta + \frac{\nabla\cdot\mathbf{v}}{R} = 0, \tag{7}$$

$$\nabla^2\psi = 4\pi R^2 G\rho_b\delta, \tag{8}$$

$$\nabla\cdot\mathbf{B}_b = \nabla\cdot\mathbf{b} = 0, \tag{9}$$

$$\partial_t(R^2\mathbf{B}_b) = 0, \tag{10}$$

$$\partial_t(R^2\mathbf{b}) = \frac{\nabla\times(\mathbf{v}\times R^2\mathbf{B}_b)}{R}. \tag{11}$$

Note that eqs. (10) and (11) allow us to clearly distinguish between the background field $\mathbf{B}_b$ and the perturbed field $\mathbf{b}$.

In addition to eqs. (6)–(11), we have a number of further constraints which depend on the cosmological model we assume. To isolate the effect of magnetic fields from other sources of density perturbation and to keep the analysis simple, we chose to study first the case of a flat universe with a critical density of baryons ($\Omega_B = 1$). In §3 and §5 we discuss the effect on our results of including non-baryonic dark matter as the dominant component of the universe.

For an Einstein–De Sitter model, the following relations hold during the time of interest ($0 \leq z \leq z_{\rm rec} \simeq 1100$):

$$\rho_b(t)R^3(t) = \rho_b(t_0) \equiv \rho_0, \tag{12a}$$

$$6\pi G\rho_b(t)t^2 = 1, \tag{12b}$$

$$R(t) = (t/t_0)^{2/3}, \tag{12c}$$

$$\mathbf{B}_b(\mathbf{x},t)R^2(t) = \mathbf{B}_{\rm rec}(\mathbf{x})R^2(t_{\rm rec}) = \mathbf{B}_b(\mathbf{x},t_0) \equiv \mathbf{B}_0(\mathbf{x})\,, \tag{12d}$$

where t_0 is the age of the universe, and quantities with subscript 0 are evaluated at the present time; we choose $R(t_0) \equiv 1$. Note that eq. (12d) follows trivially from eq. (10) above.

3. The Compressible Mode

In the following, we first derive the time evolution of the compressible modes and then solve for the spectrum of generated density perturbations. In §4 we derive the corresponding evolution for the incompressible modes, which evolve differently and are decoupled from the compressible modes.

3.1 Time Evolution

Taking the divergence and time derivative of eq. (6), and using the remaining eqs. (7)–(12), we obtain an equation for the evolution of the velocity divergence,

$$\partial_t\left\{R\,\partial_t(R\nabla\cdot\mathbf{v})\right\} - \frac{4\pi G\rho_0}{R}\nabla\cdot\mathbf{v} = \frac{\nabla\cdot\mathbf{Q}}{4\pi\rho_0 R}\,, \tag{13}$$

where

$$\mathbf{Q} \equiv [\nabla\times\nabla\times(\mathbf{v}\times\mathbf{B}_0)]\times\mathbf{B}_0 + (\nabla\times\mathbf{B}_0)\times[\nabla\times(\mathbf{v}\times\mathbf{B}_0)]\,. \tag{14}$$

Using eqs. (12), we can re-write eq. (13) in the form

$$\nabla\cdot\left(\partial_{tt}\mathbf{v} + \frac{2}{t}\partial_t\mathbf{v} - \frac{4}{9t^2}\mathbf{v}\right) = \left(\frac{t_o}{t}\right)^2\frac{\nabla\cdot\mathbf{Q}}{4\pi\rho_0}\,. \tag{15}$$

We next Fourier–transform the fluid variables in comoving coordinates,

$$\mathbf{B}_0(\mathbf{x}) = \int d^3\mathbf{k}\ \exp(i\mathbf{k}\cdot\mathbf{x})\tilde{\mathbf{B}}(\mathbf{k})\,, \tag{16}$$

$$\mathbf{v}(\mathbf{x},t) = \int d^3\mathbf{k}\ \exp(i\mathbf{k}\cdot\mathbf{x})\tilde{\mathbf{v}}(\mathbf{k},t)\,. \tag{17}$$

$\mathbf{B}_{rec}(\mathbf{x})$ is assumed to be homogeneous and isotropic (and, obviously, so is $\mathbf{B}_0(\mathbf{x})$); therefore $\tilde{\mathbf{B}}(\mathbf{k})$ obeys the relation (cf. Kraichnan & Nagarajan 1967; Moffatt 1978)

$$\langle \tilde{B}_i(\mathbf{k}_1)\tilde{B}_j^*(\mathbf{k}_2)\rangle = \delta^3(\mathbf{k}_1-\mathbf{k}_2)\left(\delta_{ij}-\frac{k_{1i}k_{2j}}{k_1^2}\right)\frac{\tilde{B}^2(k_1)}{2}\,, \tag{18}$$

where i and j label the i-th and j-th components of the vector $\tilde{\mathbf{B}}(\mathbf{k})$. The evolution equation for each velocity mode $\tilde{\mathbf{v}}(\mathbf{k})$ is then obtained by inserting the Fourier expressions (16)–(17) into eq. (15):

$$\mathbf{k}\cdot\left(t^2\partial_{tt}+2t\partial_t-\frac{4}{9}\right)\ \tilde{\mathbf{v}}(\mathbf{k},t) = \beta\int d^3\mathbf{k}_1 d^3\mathbf{k}_2\ F[\mathbf{k},\mathbf{k}_1,\mathbf{k}_2,\tilde{\mathbf{B}}(\mathbf{k}_1),\tilde{\mathbf{B}}(\mathbf{k}_2),\tilde{\mathbf{v}}(\mathbf{k}-\mathbf{k}_1-\mathbf{k}_2,t)], \tag{19}$$

where

$$\beta \equiv \frac{t_0^2}{4\pi\rho_0} = \frac{1}{24\pi^2\rho_0^2 G}\,,$$
$$F \equiv -\{k^2(\tilde{\mathbf{B}}_1\cdot\tilde{\mathbf{B}}_2)(k-k_2)_i - k^2[(\mathbf{k}-\mathbf{k}_2)\cdot\tilde{\mathbf{B}}_1]\tilde{B}_{2i}$$
$$+\,2(\mathbf{k}\cdot\tilde{\mathbf{B}}_2)[(\mathbf{k}\cdot\tilde{\mathbf{B}}_1)k_{2i}-(\mathbf{k}_2\cdot\tilde{\mathbf{B}}_1)k_i]\}\,\tilde{v}_i(\mathbf{k}-\mathbf{k}_1-\mathbf{k}_2,t)\,,$$

$\tilde{\mathbf{B}}_1 \equiv \tilde{\mathbf{B}}(\mathbf{k}_1)$, and $\tilde{\mathbf{B}}_2 \equiv \tilde{\mathbf{B}}(\mathbf{k}_2)$. For notational convenience, we define a logarithmic time variable $T \equiv \ln t$, and further define the operator G_i such that

$$\int d^3\mathbf{k}_1 d^3\mathbf{k}_2\ F \equiv G_i(\mathbf{k}:\mathbf{l})v_i(\mathbf{l},T)\,,$$

i.e.,

$$G_i \equiv -\int d^3\mathbf{k}_1 d^3\mathbf{k}_2 d^3\mathbf{l}\{k^2(\tilde{\mathbf{B}}_1\cdot\tilde{\mathbf{B}}_2)(k-k_2)_i - k^2[(\mathbf{k}-\mathbf{k}_2)\cdot\tilde{\mathbf{B}}_1]\tilde{B}_{2i}$$
$$+\,2(\mathbf{k}\cdot\tilde{\mathbf{B}}_2)[(\mathbf{k}\cdot\tilde{\mathbf{B}}_1)k_{2i}-(\mathbf{k}_2\cdot\tilde{\mathbf{B}}_1)k_i]\}\,\delta(\mathbf{k}-\mathbf{k}_1-\mathbf{k}_2-\mathbf{l})\,.$$

Upon using the definition $\mathbf{k}\cdot\tilde{\mathbf{v}}(\mathbf{k},t) = k\tilde{v}_{\|}(\mathbf{k},t)$, where the subscript $\|$ represents the compressible (longitudinal) component of $\tilde{\mathbf{v}}$, eq. (19) then reads

$$\left(\partial_{TT}+\partial_T-\frac{4}{9}\right)\ \tilde{v}_{\|}(\mathbf{k},T) = \frac{\beta}{k}G_i(\mathbf{k}:\mathbf{l})\tilde{v}_i(\mathbf{l},T)\,. \tag{20}$$

Since the ensemble average of both sides of eq. (20) vanishes, we compute the evolution of the quadratic quantities. At the expense of yet further algebra, one obtains the following three equations:

$$\partial_T\langle|\tilde{v}_\parallel(\mathbf{k},T)|^2\rangle = 2Re\langle\tilde{v}_\parallel(\mathbf{k},T)\partial_T\tilde{v}^*_\parallel(\mathbf{k},T)\rangle\,, \tag{21a}$$

$$\begin{aligned}\partial_T Re\langle\tilde{v}_\parallel(\mathbf{k},T)\partial_T\tilde{v}^*_\parallel(\mathbf{k},T)\rangle &= \frac{4}{9}\langle|\tilde{v}_\parallel(\mathbf{k},T)|^2\rangle - Re\langle\tilde{v}_\parallel(\mathbf{k},T)\partial_T\tilde{v}^*_\parallel(\mathbf{k},T)\rangle \\ &+\langle|\partial_T\tilde{v}_\parallel(\mathbf{k},T)|^2\rangle + \frac{\beta}{k}Re\langle G_i(\mathbf{k}:\mathbf{l})\tilde{v}_i(\mathbf{l},T)\tilde{v}^*_\parallel(\mathbf{k},T)\rangle\,, \end{aligned}\tag{21b}$$

$$\begin{aligned}\partial_T\langle|\partial_T\tilde{v}_\parallel(\mathbf{k},T)|^2\rangle &= \frac{8}{9}Re\langle\tilde{v}_\parallel(\mathbf{k},T)\partial_T\tilde{v}^*_\parallel(\mathbf{k},T)\rangle - 2\langle|\partial_T\tilde{v}_\parallel(\mathbf{k},T)|^2\rangle \\ &+\frac{2\beta}{k}Re\langle G_i(\mathbf{k}:\mathbf{l})\tilde{v}_i(\mathbf{l},T)\partial_T\tilde{v}^*_\parallel(\mathbf{k},T)\rangle\,, \end{aligned}\tag{21c}$$

where Re stands for the real part. These equations look more complex than they really are because the recurring term $\langle Gvv^*\rangle$ can be calculated easily if one notes that $\langle B\tilde{v}(T)\rangle$ and $\int G\langle v_\parallel v_\perp\rangle$ vanish (see Appendix A). Thus,

$$\langle G_i(\mathbf{k}:\mathbf{l})\tilde{v}_i(\mathbf{l})\tilde{v}^*_\parallel(\mathbf{k})\rangle = -\frac{2}{3}\langle B_0^2\rangle k^3\langle|\tilde{v}_\parallel(\mathbf{k})|^2\rangle\,.$$

and

$$\langle G_i(\mathbf{k}:\mathbf{l})\tilde{v}_i(\mathbf{l})\partial_T\tilde{v}^*_\parallel(\mathbf{k})\rangle = -\frac{2}{3}\langle B_0^2\rangle k^3\langle\tilde{v}_\parallel(\mathbf{k})\partial_T\tilde{v}^*_\parallel(\mathbf{k})\rangle\,,$$

where

$$\langle B_0^2\rangle \equiv \int dk\ 4\pi k^2\tilde{B}^2(k)\,.$$

These considerations allow us to write a single evolution equation for $\langle|\tilde{v}_\parallel(\mathbf{k},T)|^2\rangle$,

$$\left\{\partial_{TTT} + 3\partial_{TT} + \left(\frac{2}{9}+\frac{4}{3}ak^2\right)\partial_T + \left(\frac{4}{3}ak^2 - \frac{16}{9}\right)\right\}\langle|\tilde{v}_\parallel(\mathbf{k},T)|^2\rangle = 0\,. \tag{22}$$

where

$$a \equiv 2\beta\langle B_0^2\rangle = \frac{\langle B_0^2\rangle}{12\pi^2\rho_0^2 G}\,.$$

In addition, we have the initial conditions (at $T = T_{\rm rec}$):

$$\begin{aligned}\langle\tilde{v}_\parallel(\mathbf{k},T=T_{\rm rec})\rangle &= 0\,,\\ \partial_T\langle|\tilde{v}_\parallel(\mathbf{k},T)|^2\rangle|_{T_{\rm rec}} &= 2Re\langle\tilde{v}_\parallel(\mathbf{k},T_{\rm rec})\partial_T\tilde{v}^*_\parallel(\mathbf{k},T_{\rm rec})\rangle = 0\,,\\ \partial_{TT}\langle|\tilde{v}_\parallel(\mathbf{k},T)|^2\rangle|_{T=T_{\rm rec}} &= 2\langle|\partial_T\tilde{v}_\parallel(\mathbf{k},T_{\rm rec})|^2\rangle = 2\left[t_{\rm rec}\,\dot{v}_{\parallel,{\rm rms}}(k,t_{\rm rec})\right]^2\,,\end{aligned}$$

where $\dot{v} \equiv \partial_t v$ and $\tilde{v}_{\|,\mathrm{rms}}(k,t) \equiv \sqrt{\langle|\tilde{v}_{\|}(\mathbf{k},t)|^2\rangle}$. These follow from the assumption that the velocity is zero everywhere at $t = t_{\mathrm{rec}}$. In the last initial condition above, $\dot{\tilde{v}}_{\|,\mathrm{rms}}(k, t_{\mathrm{rec}})$ will be obtained later upon using eq. (6).

Returning to our original time variable $t \equiv \exp(T)$, and again defining time derivatives with respect to the ordinary time t, the solution for the *rms* velocity can be written as follows:

(i) For $k \neq k_B$:

$$\tilde{v}_{\|,\mathrm{rms}}(k,t) = \dot{\tilde{v}}_{\|,\mathrm{rms}}(k,t_{\mathrm{rec}})\frac{3t_{\mathrm{rec}}}{m}\left(\frac{t}{t_{\mathrm{rec}}}\right)^{-\frac{1}{2}}\left[\left(\frac{t}{t_{\mathrm{rec}}}\right)^{\frac{m}{6}} - \left(\frac{t}{t_{\mathrm{rec}}}\right)^{-\frac{m}{6}}\right], \tag{23a}$$

(ii) For $k = k_B$:

$$\tilde{v}_{\|,\mathrm{rms}}(k,t) = \dot{\tilde{v}}_{\|,\mathrm{rms}}(k,t_{\mathrm{rec}})t_{\mathrm{rec}}\left(\frac{t}{t_{\mathrm{rec}}}\right)^{-\frac{1}{2}}\ln\left(\frac{t}{t_{\mathrm{rec}}}\right), \tag{23b}$$

where $m(k) \equiv \sqrt{25 - 12ak^2} = 5\sqrt{1 - (k/k_B)^2}$. The transition from stable ($m^2 < 0$) to unstable ($m^2 > 0$) modes occurs at $k = k_B$, and we therefore find the magnetic Jeans length to be

$$\lambda_B \equiv \frac{2\pi}{k_B} = 2\pi\sqrt{\frac{12a}{25}} = \frac{2}{5}\frac{\langle B_0^2\rangle^{1/2}}{\rho_0\sqrt{G}} . \tag{24}$$

Modes with length scales greater than λ_B ($k < k_B$) are unstable, while those on scales smaller than λ_B ($k > k_B$) undergo damped oscillations. As in Peebles (1980, 1993), one can roughly estimate the magnetic Jeans length by using the Alfvén speed, $v_A = B/\sqrt{4\pi\rho}$, in place of the sound speed in the expression for the ordinary Jeans length, which gives

$$\lambda_B \sim \frac{B}{2\rho}\frac{1}{\sqrt{G}},$$

very close to the exact expression derived in eq. (24).

The magnetic Jeans length derived above can be constrained by the requiring that, at the time of nucleosynthesis, the average energy density in the magnetic field,

$$\rho_B(t) = \frac{\langle \mathbf{B}(\mathbf{x},t)^2\rangle}{8\pi} = \frac{\langle B_0^2\rangle}{8\pi R(t)^4} .$$

be significantly less than the energy density in radiation,

$$\rho_r(t) = \frac{\pi^2 g_* T^4}{30} ,$$

where g_* is the number of relativistic degrees of freedom. and T is the temperature of the background radiation (Barrow 1976). Since both energy densities redshift as R^{-4}, it suffices to require that $\rho_B \ll \rho_r$ today. which gives:

$$\langle B_0^2 \rangle^{\frac{1}{2}} \ll 4 \times 10^{-6} \text{ Gauss} .$$

In principle, we should also take into account the limit on the fraction of the critical density in baryons given by primordial nucleosynthesis, $\Omega_B h^2 \leq 0.015$ (Walker et al. 1991), but we have assumed a critical baryon dominated universe in deriving our solutions. For self-consistency, we choose to omit factors of Ω_B in the present manuscript and leave it for a subsequent paper where non-baryonic dark matter is included. (We also set $h = 1$ unless it is indicated explicitly.) By assuming a critical density in baryons, $\rho_0 \simeq 2 \times 10^{-29}$ g cm^{-3}, in eq. (24), we can write:

$$k_B \simeq \frac{2\pi}{100 \text{ Mpc}} \left(\frac{4 \times 10^{-6} \text{Gauss}}{\langle B_0^2 \rangle^{\frac{1}{2}}} \right) . \tag{25}$$

Therefore, the constraint $\rho_B \ll \rho_r$ implies that the magnetic Jeans length today must satisfy $\lambda_B(t_0) \ll 100$ Mpc, i.e.,

$$k_B \gg \frac{2\pi}{100\text{Mpc}} . \tag{26}$$

(Note that if we had set $\Omega_B < 1$ in the density used in eq. (25), the effect would be to increase the maximum λ_B, thus weakening the constraint.)

It is interesting to note that, unlike the ordinary Jeans length, λ_B is fixed in comoving coordinates; for $t_0 > t > t_{\text{rec}}$, $\lambda_B(t) = \lambda_B(t_0)R(t)$.

We can now solve for

$$\tilde{\delta}_{\text{rms}}(k,t) \equiv \sqrt{\langle |\tilde{\delta}(\mathbf{k},t)|^2 \rangle}$$

by using the corresponding solution $\tilde{v}_{\text{rms}}(k,t)$, with the initial condition

$$\tilde{\delta}_{\text{rms}}(k, t_{\text{rec}}) = 0 ,$$

and eq. (7). The detailed derivation of $\tilde{\delta}_{\text{rms}}(k,t)$ as a function of $\tilde{v}_{\text{rms}}(k,t)$ is provided in Appendix B; here we only write the solution,

$$\tilde{\delta}_{\text{rms}}(k,t) \equiv c(k)\tau(k,t)$$

where, for $k \neq k_B$.

$$\tau(k,t) = \frac{18}{m^2-1}\left[\left[1+\frac{1}{m}\right]\left(\frac{t}{t_{\rm rec}}\right)^{\frac{m-1}{6}} + \left[1-\frac{1}{m}\right]\left(\frac{t}{t_{\rm rec}}\right)^{-\frac{(m+1)}{6}} - 2\right], \tag{27a}$$

for $k = k_B$,

$$\tau(k,t) = 36\left(\frac{t}{t_{\rm rec}}\right)^{-\frac{1}{6}}\left[\left(\frac{t}{t_{\rm rec}}\right)^{\frac{1}{6}} - 1 - \frac{1}{6}\ln\left(\frac{t}{t_{\rm rec}}\right)\right], \tag{27b}$$

and

$$c(k) = \frac{{t_{\rm rec}}^2}{R_{\rm rec}}\,\dot{\tilde{v}}_{\parallel,{\rm rms}}(k,t_{\rm rec})\,k\,. \tag{28}$$

In the form for $\tilde{\delta}_{\rm rms}(k,t)$ defined above, $\tau(k,t)$ can be thought of as a transfer function which evolves an initial spectrum $c(k)$ from recombination to a later time t. We now discuss the behaviour of $\tau(k,t)$ and leave a discussion of $c(k)$, which depends on the particular form of the magnetic field spectrum, to the next section (§3.2).

An interesting feature of the solution is that $\tau(k,t)$ is independent of the spectrum of the magnetic field (as long as it is Gaussian distributed) and only depends on the combinations k/k_B and $t/t_{\rm rec}$. Therefore, the solution can be easily rescaled for different choices of magnetic field strength. The time evolution reduces to the usual $t^{2/3}$ growing and t^{-1} decaying modes in the limit $k/k_B \to 0$. For $k/k_B \ll 1$ so that $m \simeq 5$, the growth of perturbations is nearly independent of k, so that the final spectrum is mostly proportional to the initial spectrum given by $c(k)$. As $k \to k_B$ from below, the growth of perturbations decreases and. at $k = k_B$, the solution changes from unstable (for $k < k_B$) to damped oscillatory (for $k > k_B$).

In principle, the time evolution derived above is only valid for modes which correspond to scales smaller than the Hubble radius at recombination, $k > k_{\rm rec} \simeq 2\pi/100$ Mpc. Modes on comoving scales between the Hubble radius at recombination and the Hubble radius today have similar but delayed time evolution, since these modes start growing after they enter the Hubble radius. As we show below, the spectrum of perturbations, $c(k)$, is fairly steep for small k, so that the power for small k modes is negligible, and we can approximate the power for $k < k_{\rm rec}$ to be zero. Alternatively, we can estimate the effect of the delayed evolution by using $t/t_{\rm enter}(k)$ instead of $t/t_{\rm rec}$ in $\tau(k,t)$ for modes with $k < k_{\rm rec}$, where $t_{\rm enter}(k)$ is the time a k-mode enters the Hubble radius, $t_{\rm enter}(k) = t_{\rm rec}(k_{\rm rec}/k)^3$.

In Fig. 1, we plot $\tau(k,t/t_{\rm rec})$ for $k > k_{\rm rec}$ and $\tau(k,t/t_{\rm enter})$ for $k < k_{\rm rec}$ at different redshifts. (The sharp discontinuity at $k_{\rm rec}$ is an artifact of the approximation that recombination happened instantaneously.) We can see that, independent of the spectrum of the magnetic field, the power on scales $k \leq k_{\rm rec}$ is supressed (by the delayed growth) as is the power on scales $k \geq k_B$. Therefore, while magnetic fields do not generate significant clustering on scales larger than $\sim 2\pi k_{\rm rec}^{-1}$ and smaller than $\sim 2\pi k_B^{-1}$, they can have significant influence on the formation of structure between these two scales, depending on the strength and spectrum of magnetic fields at recombination.

If the universe were baryon–dominated with infinite conductivity, magnetic fields could deter the growth of perturbations on scales smaller than λ_B; hence, a constraint on the strength of magnetic fields could be derived by the observation that structures do form on a given scale above the ordinary Jeans length λ_J. For example, for galaxies to form in a baryon–dominated, infinitely conducting flat universe, we would require $\lambda_B \lesssim l_g \simeq 1$ Mpc and, therefore, $\langle B_0^2\rangle^{1/2} \lesssim 4 \times 10^{-8}$ Gauss. However, this result does not take into account the presence of neutral hydrogen or non-baryonic dark matter. When these components are present, modes on scales below λ_B are also unstable.

A stronger constraint on the strength of magnetic fields in the Universe comes from the observation that the large scale magnetic field in our Galaxy is ~ 3 μGauss. If the observed galactic magnetic field were solely due to a primordial field enhanced by the collapse of the Galaxy, then the average field in the universe on the scale l_g (the comoving scale that collapsed to form a galaxy) would be $\bar{B}_0(l_g) \lesssim 10^{-9}$ Gauss (using 2×10^{-24}g cm^{-3} for the average gas density in the Galaxy, 2×10^{-29}g cm^{-3} for the average gas density in the Universe, and the assumption that the field is frozen in as the gas contracts, $B \propto \rho^{2/3}$). This limit cannot be unambiguously translated into a limit on $\langle B_0^2\rangle$ since $\bar{B}_0(l_g)$ refers to the average field on a particular scale l_g averaged with a window function. This averaging procedure depends not only on the integrated power spectrum $\langle B_0^2\rangle$, but on the power spectrum $\tilde{B}^2(k)$ as well, unless $\langle B_0^2\rangle \lesssim 10^{-9}$ Gauss. We return to this constraint during our discussion of magnetic field spectra below.

3.2 The Perturbation Spectrum

In order to obtain the spectral dependence, $\dot{\tilde{v}}_{\rm rms}(k, t_{\rm rec})$ or $c(k)$, we need to assume a specific spectrum for the background magnetic field at recombination, and solve eq. (6) at $t_{\rm rec}$:

$$\nabla \cdot \dot{\mathbf{v}}(\mathbf{x}, t_{\rm rec}) = \frac{\nabla \cdot [(\nabla \times \mathbf{B}_{\rm rec}) \times \mathbf{B}_{\rm rec}]}{4\pi\rho_b(t_{\rm rec})R_{\rm rec}} = \frac{\nabla \cdot [(\nabla \times \mathbf{B}_0) \times \mathbf{B}_0]}{4\pi\rho_0 R_{\rm rec}^2}. \qquad (29)$$

Since a given k-mode of the velocity field is a non-linear convolution of the magnetic field spectrum, different k-modes of $\tilde{B}(k)$ will contribute to a given mode of $\tilde{v}(k)$. In particular, if the spectrum for the magnetic field has an ultraviolet cutoff, $k_{\max}$, the velocity field modes will be non-zero for $k \leq 2k_{\max}$. Therefore, the highest k-mode for the growing density perturbations will be $\min(2k_{\max}, k_B)$. In principle, the lowest k-mode excited through eq.(29) is $k = 0$, even if the magnetic field spectrum has an infrared cutoff. but, in practice, the Hubble radius at each time will provide an effective infrared cutoff for the density perturbations excited by the magnetic field. As we show below, the power in low k-modes is too small for the infrared cutoff to be relevant.

In what follows, we discuss two Ansätze for the functional form of the magnetic field spectrum: power laws and delta functions. The delta function Ansatz is simple to calculate, and can be used to relate our results to those of Wasserman (1978) and to the more realistic case of the power law Ansatz.

3.2.1 Delta Function Spectra for $\tilde{B}^2(k)$

If the magnetic field spectrum at recombination is a delta function, we can write

$$\tilde{B}^2(k) \equiv A\frac{\delta(k-k_*)}{4\pi k^2}. \tag{30}$$

where A is a constant ($A = \langle B_0^2\rangle$ by the definition of $\langle B_0^2\rangle$), the initial acceleration becomes for $k \leq 2k_*$ (see Appendix C for details)

$$\dot{\tilde{v}}_{\|,\mathrm{rms}}(k, t_{\mathrm{rec}}) = \sqrt{V}\frac{\langle B_0^2\rangle}{(4\pi)^3\rho_0 R_{\mathrm{rec}}^2}\frac{k^{\frac{1}{2}}}{k_*} \tag{31}$$

where V is a volume factor. Using eq. (28) and the definition of k_B, we find for the "initial" density spectrum

$$c(k) = \frac{25\sqrt{V}}{384\pi^2}\frac{k^{\frac{3}{2}}}{k_B^2 k_*}. \tag{32}$$

We can now calculate the power spectrum of density perturbations, $P(k,t)$. and the variance (*rms* power per logarithmic wavenumber interval), $\Delta(k,t)$ using the following definitions

$$P(k,t) \equiv \frac{(2\pi)^3}{V}\langle|\tilde{\delta}(k,t)|^2\rangle \tag{33}$$

such that,

$$\langle|\delta(\mathbf{x},t)|^2\rangle \equiv \int d^3\mathbf{k}P(k,t),$$

and

$$\Delta(k,t)^2 \equiv 4\pi k^3 P(k,t) = \frac{32\pi^4}{V}k^3\langle|\tilde{\delta}(k,t)|^2\rangle \tag{34}$$

such that,

$$\langle|\delta(\mathbf{x},t)|^2\rangle \equiv \int \Delta(k,t)^2 d\ln k\,.$$

For the delta function magnetic field spectrum, we obtain

$$\Delta_\delta(k,t) = \frac{25\sqrt{2}}{96}\left(\frac{k}{k_B}\right)^3 \frac{k_B}{k_*}\,\tau(k,t)\,. \tag{35}$$

In Fig. 2, we plot $\Delta_\delta(k,t)/(k_B/k_*)$ at different redshifts, asssuming $k_* > k_B/2$. We rescale the amplitude by k_B/k_* so that any choice of k_* is represented as long as $k_* > k_B/2$. For $k_* < k_B/2$, the result is the same for wavenumbers $k < k_*$, but, because of the cutoff at $2k_*$, Δ_δ is zero for $k > 2k_*$. For small k, both P_δ and $\Delta_\delta \propto k^3$ for $k \gtrsim k_{\rm rec}$ and steeper for $k < k_{\rm rec}$, while the peak power occurs at $k \sim \min(k_B, 2k_*)$.

The resulting power spectrum of magnetic field-generated density perturbations can be compared to observations of galaxy clustering, if we assume that galaxies trace the mass density distribution. The power spectrum of galaxy clustering has been measured over the range 0.1 Mpc $\lesssim 2\pi k^{-1} \lesssim 10^2$ Mpc (e.g., Geller & Huchra 1989; Efstathiou et al. 1990; Maddox et al. 1990; Collins, Nichol, & Lumsden 1992; Fisher et al. 1993), while information from anisotropies in the background radiation reaches scales comparable to the present Hubble radius $k_0 \simeq 2\pi/3 \times 10^3$ Mpc (Smoot et al. 1992; Ganga, Cheng, Meyer, & Page 1993). In the absence of bias, an estimate of the present-day scale of non-linear clustering can be made by estimating the scale at which the *rms* galaxy fluctuations are unity; for optically selected galaxies this is $l_{nl}(t_0) \simeq 8h^{-1}$ Mpc. On large scales ($0.01{\rm Mpc}^{-1} < k < k_{nl}$), the observed galaxy power spectrum is consistent with a power law, $P(k) \propto k^n$, $n \simeq -1$ with a hint of a bend to larger n at the larger scales. COBE suggests that $P(k) \propto k$ on the largest scales. Therefore, magnetic field-induced perturbations (with a delta function magnetic field spectrum) have too steep a spectrum ($P_\delta(k) \propto k^3$) to agree with observations on large scales. As we discuss below, a similar behaviour is found if $\tilde{B}^2(k)$ is a power law (in that case, $P(k) \propto k^4$); therefore, magnetic field-induced density perturbations *cannot* reproduce the observations of structure on large scales.

On smaller scales ($k \gtrsim 2\pi/\lambda_{nl}(t_0)$), magnetic field-induced perturbations may play an important role. In particular, they are of interest if $\tilde{B}^2(k)$ is such that $\Delta(k,t_0)_\delta \gtrsim 1$ for cosmologically relevant scales, say between clusters of galaxies ($k_{cl} \simeq 2\pi/2$ Mpc) and globular clusters ($k_{gl} \simeq 2\pi/10^{-2}$ Mpc). As $\Delta_\delta(k,t)$ approaches 1, the linear treatment used above breaks down. However, we can make use of our linear solution to approximately estimate the epoch, $t_{nl}(k)$, that a particular scale k becomes non-linear by setting $\Delta_\delta(k, t_{nl}(k)) \simeq 1$ in eq. (35).

To see whether magnetic fields can generate non-linear structure, we must apply the general observational constraints upon the field for the case of a delta function spectrum. As discussed at the end of §3.1, the observed galactic field implies that the average field on scales $l \sim l_g$ must be less than 10^{-9} Gauss. Define the average field on scale l by

$$\begin{aligned} \bar{B}^2(l,t) &\equiv \langle\left(\int d^3x\, \mathbf{B}(\mathbf{x},t) W(\mathbf{x}-\mathbf{x}')\right)^2\rangle_{\mathbf{x}'} \\ &= \int d^3k\, \tilde{B}^2(k,t)|W(kl)|^2 \quad , \end{aligned} \tag{36}$$

where $W(\mathbf{x}-\mathbf{x}')$ is a window function which smooths the magnetic field on scale l and $W(kl)$ is its Fourier transform. The observed galactic field constrains $\bar{B}(l_g, t_0) \lesssim 10^{-9}$ Gauss. Using a Gaussian window function, $W(\mathbf{x}-\mathbf{x}') = \exp(-|\mathbf{x}-\mathbf{x}'|^2/2l^2)$ in eq. (36), we find

$$\bar{B}(l,t_0) = \langle B_0^2\rangle^{\frac{1}{2}} \exp(-\frac{k_*^2 l^2}{2}) .$$

Obviously. $\bar{B}(l,t_0) \leq \langle B_0^2\rangle$ and for $l = l_g \simeq 1$ Mpc with the help of eq. (25), we can write

$$k_*^2 \geq \frac{2}{l_g^2} \ln\left(\frac{2\pi/25\text{kpc}}{k_B}\right) , \tag{37}$$

which is not an easily implemented constraint because there are only upper limits for both $\langle B_0^2\rangle$ and $\bar{B}(l_g, t_0)$. When we discuss particular examples below, we implement this constraint case by case.

We now discuss what ranges of magnetic field scales k_* and strength k_B (or $\langle B_0^2\rangle$) are relevant for structure formation. The time evolution of Δ implies that just after recombination perturbations on small scales grow faster than larger scales. Therefore. if non-linear structures form early. the first scales to become non-linear have $k \sim k_> \equiv \min(2k_*, k_B)$. We can then solve for time, $t_{nl}(k_>)$, when $\Delta(k_>, t_{nl}(k_>)) = 1$. For $2k_* > k_B$, setting $\Delta_\delta(k_B, t_{nl}) \simeq 1$ we find that t_{nl} satisfies

$$\left(\frac{t_{nl}}{t_{\text{rec}}}\right)^{\frac{1}{3}} (1-\gamma_\delta) = 1 + \frac{1}{6}\ln\left(\frac{t_{nl}}{t_{\text{rec}}}\right) , \tag{38}$$

where $\gamma_\delta = 7.54 \times 10^{-2} k_*/k_B$. Since $t_{nl} \to t_{\rm rec}$ as $\gamma_\delta \to 0$, the closer k_* is to $k_B/2$, the earlier non-linear structure on scale k_B can form.

For example, if we take $k_* = k_B$, then $t_{nl}(k_B) \simeq 15\, t_{\rm rec}$, and perturbations on scale k_B become non-linear at redshift $z_{nl}(k_B) \simeq 180$. For this choice of k_*, structure would become non-linear today on scales $k_{nl}(t_0) \simeq 0.14\, k_B$ (see eq. (39) below). If we set $k_{nl}(t_0) = 2\pi/8$ Mpc, then $k_* = k_B \simeq 2\pi/1$ Mpc. These choices satisfy both constraints from eq. (26) and eq. (37), with $\langle B_0^2 \rangle^{1/2} \simeq 4 \times 10^{-8}$ Gauss and $\bar{B}(l_g, t_0) \simeq 2 \times 10^{-12}$ Gauss.

As k_*/k_B increases from unity, $t_{nl}(k_B)$ increases and eventually approaches t_0 for $k_* = 7k_B$. Therefore, k_* must be less than $7k_B$ for magnetic fields (with a delta function power spectrum) to play a role in structure formation.

As k_*/k_B decreases from unity, $t_{nl}(k_B)$ drops until $k_* = k_B/2$, when the cutoff density spectrum becomes $2k_*$ instead of k_B. For $k_* < k_B/2$, we need to follow $t_{nl}(2k_*)$ instead to find when the first objects form. To find $t_{nl}(k)$ for any $k \ll k_B$, we can approximate $m \simeq 5$ in eq. (27a) and write:

$$\left(\frac{t_{nl}(k)}{t_{\rm rec}}\right)^{\frac{2}{3}} \simeq 3\frac{k_*}{k_B}\left(\frac{k_B}{k}\right)^3 . \tag{39}$$

Using eq. (39), we find the time at which perturbations with $k = 2k_*$ become non-linear, $t_{nl}(2k_*) \simeq 1.8\, t_{\rm rec}\, (k_B/2k_*)^3$. Requiring that $t_{nl}(2k_*) \le t_0$ implies $2k_* \gtrsim 3.7 \times 10^{-2} k_B$. For example, suppose $2k_* = 0.1 k_B$, which gives $t_{nl}(2k_*) \simeq 1.8 \times 10^3 t_{\rm rec}$ or redshift $z_{nl}(2k_*) \simeq 6$. In this case, choosing the galaxy scale to go non-linear at $z \simeq 6$, we get $2k_* \simeq 2\pi/1$ Mpc, $k_B \simeq 2\pi/0.1$ Mpc, and the constraints eq. (26) and eq. (37) are satisfied with $\langle B_0^2 \rangle^{1/2} \simeq 4 \times 10^{-9}$ Gauss and $\bar{B}(l_g, t_0) \simeq 3 \times 10^{-11}$ Gauss. This scenario would correspond to the formation of galaxies around redshift 6. (Note that if we chose instead $t_{nl}(2k_*) = t_0$ and $2k_* = 2\pi/8$ Mpc, then $k_B = 2\pi/0.3$ Mpc, which satisfies eq. (26) but violates eq. (37).

The examples discussed above demonstrate how non-linear structures within a limited but relevant range of scales can be formed at reasonable redshifts if magnetic fields satisfying observational limits were present at recombination. Because of the steep spectrum, the scales influenced by magnetic fields are primarily in the non-linear regime, ultimately requiring a detailed numerical study. Although the Ansatz used above for the magnetic field spectrum is not realistic, some of the results obtained above are very similar to the power-law spectrum discussed below.

Before leaving this section, we note that Wasserman (1978) discussed the case in which

$\tilde{B}^2(k)$ is sharply peaked around $k = 2\pi/x_G$ (his x_G corresponds to our l_g) and wrote (his eq. (26))

$$\langle|\nabla\cdot[(\nabla\times\mathbf{B}_{\rm ret})\times\mathbf{B}_{\rm rec}]|^2\rangle^{\frac{1}{2}} \sim \left(\frac{4}{3}\right)^{\frac{1}{2}}\left(\frac{2\pi}{x_G}\right)^2\langle B^2_{\rm rec}(x)\rangle\,,$$

as an estimate of the effect of magnetic fields. His result corresponds to an average over the volume

$$\langle|\nabla\cdot[(\nabla\times\mathbf{B}_{\rm rec})\times\mathbf{B}_{\rm rec}]|^2\rangle = \frac{(4\pi\rho_b(t_{\rm rec})R_{\rm rec})^2}{V}\int d^3\mathbf{x}\langle|\nabla\cdot\dot{\mathbf{v}}(\mathbf{x},t)|^2\rangle$$

which, through Parseval's theorem, can be re-written as

$$\langle|\nabla\cdot[(\nabla\times\mathbf{B}_{\rm rec})\times\mathbf{B}_{\rm rec}]|^2\rangle = \frac{(4\pi\rho_b(t_{\rm rec})R_{\rm rec})^2}{V}(2\pi)^3\int d^3\mathbf{k}\langle|\mathbf{k}\cdot\dot{\mathbf{v}}(\mathbf{k},t)|^2\rangle\,.$$

Choosing $k_* = 2\pi/x_G$ in the delta function Ansatz for $\tilde{B}^2(k)$ and using eq. (31), we recover Wasserman's eq. (26).

3.2.1 Power Law Spectra for $\tilde{B}^2(k)$

A variety of mechanisms for generating magnetic fields before recombination have been proposed (Hogan 1983; Turner & Widrow 1988; Quashnock, Loeb, & Spergel 1989; Vaschaspati 1991; Ratra 1993; Cheng & Olinto 1994), but consensus on a well–motivated scenario is still lacking. In general, most models generate a power law spectrum, $\tilde{B}^2(k) \propto k^n$, with a cutoff on small scales (a typical cutoff scale is some fraction of the Hubble radius when the field was generated). Of particular interest is the case of a white noise ($n = 0$) spectrum, which would result from magnetic fields generated with similar strengths but random directions within each Hubble volume during a phase transition in the early universe (e.g., Hogan 1983). After the phase transition, this can be viewed as a random walk of field lines, with stepsize of the order of the coherence length (the Hubble radius at the phase transition, or some fraction of it).

The magnetic field spectrum generated in the early universe will evolve differently on different scales. On very large scales, the field is frozen into the fluid and only redshifts with the expansion of the universe, $B \propto R^{-2}$. On very small scales, the finite plasma conductivity allows diffusion of the field within the plasma. On intermediate scales, damping of the magnetohydrodynamic modes as the neutrinos decouple and later as the photons decouple will change the effective cutoff at recombination. (We are presently investigating the effects of damping due to the incomplete coupling between neutrinos and the hot plasma and between photons and baryons in the presence of magnetic fields.) Here, we restrict our attention to the evolution starting at recombination for a magnetic field spectrum parametrized by the power law index n and an ultraviolet cutoff $k_{\rm max}$.

If we assume that for $k \leq k_{\rm max}$

$$\tilde{B}^2(k) \equiv A\, k^n\,, \tag{40}$$

where A is a constant, we can calculate $\dot{v}_{\|,{\rm rms}}(k, t_{\rm rec})$. To calculate it analytically, we make the further assumption that the magnetic field is Gaussian distributed. The details of the tedious algebra are left to Appendix C. To leading order in $k/k_{\rm max} \ll 1$ and for integer spectral index n between -1 and 6, we obtain the generic result that

$$\dot{v}_{\|,{\rm rms}}(k, t_{\rm rec}) \simeq \sqrt{V}\; 2\epsilon_n \frac{\langle B_0^2 \rangle}{(4\pi)^3 \rho_0 R_{\rm rec}^2} \frac{k}{k_{\rm max}^{\frac{3}{2}}}\,, \tag{41}$$

where

$$\epsilon_n \equiv \frac{\sqrt{22}(n+3)}{2\sqrt{15(2n+3)}}\,.$$

Using eq. (41), we find

$$c(k) = \frac{25\sqrt{V}}{192\pi^2} \frac{\epsilon_n k^2}{k_B^2 k_{\rm max}^{\frac{3}{2}}}\,,$$

$$\Delta_n(k,t) \simeq \frac{25\sqrt{2}}{48} \epsilon_n \left(\frac{k}{k_B}\right)^{\frac{7}{2}} \left(\frac{k_B}{k_{\rm max}}\right)^{\frac{3}{2}} \tau(k,t)\quad , \tag{42a}$$

and

$$P_n(k,t) \simeq \left(\frac{25}{48}\right)^2 \frac{\epsilon_n^2}{2\pi k_{\rm max}^3} \left(\frac{k}{k_B}\right)^4 \tau(k,t)^2\,. \tag{42b}$$

The spectrum of generated density perturbations is almost independent of the magnetic field spectral index: $\epsilon_n \simeq 1$ for $-1 \leq n \leq 6$. In contrast, there is a strong dependence on the ultraviolet cutoff $k_{\rm max}$, which plays a role similar to k_* in the delta function Ansatz. As expected, the perturbation amplitude is determined by k_B and $k_{\rm max}$. For the power-law indices discussed above, the dependence on an infrared cutoff, $k_{\rm min}$, is negligible unless $k_{\rm min}$ is larger than the wavenumber of interest.

We plot $\Delta_n(k,t)/(\epsilon_n(k_B/k_{\rm max})^{1.5})$ at different redshifts in Fig. 3, asssuming $k_{\rm max} > k_B/2$. Again, the result should be cutoff at $\sim 2k_{\rm max}$, if $2k_{\rm max} < k_B$, so that modes above $2k_{\rm max}$ have no power. (Note that the exact behaviour around $k \sim 2k_{\rm max}$ cannot be obtained from our solution, since we neglected terms of higher order in$k/k_{\rm max}$.)

For small k, $P_n \propto k^4$ for $k > k_{\rm rec}$ and is steeper for $k < k_{\rm rec}$, while the peak power is at $k \sim \min(k_B, 2k_{\rm max})$. The position of the peak is displaced logarithmically in time. An interesting property of the spectrum P_n is that, unlike the case of the delta function Ansatz, $P_n(k_B)$ does not depend on k_B. This implies that for $k_{\rm max} > k_B/2$ and $k > k_{\rm rec}$, P_n has a fixed shape and amplitude as k_B is changed, only shifting horizontally on a P_n vs. k plot.

Before exploring the relevant ranges in $k_{\rm max}$ and k_B for the formation of structure, as before we discuss the observational constraints on both parameters. The constraint on k_B in eq. (26) is unchanged, since it is independent of the magnetic field power spectrum, while the constraint on $k_{\rm max}$ depends on the spectral index n. For $n = 0$, the average field on scales l is given by (from eqs. (36) and (40)),

$$\bar{B}(l, t_0) = \sqrt{\frac{3\sqrt{\pi}}{4} \frac{\langle B_0^2 \rangle}{k_{\rm max}^3 l^3}} \,, \tag{43}$$

where we use the same Gaussian window function as in the previous section to smooth the field on galactic scales. Again, for $l = l_g$, $\bar{B}(l_g, t_0) \lesssim 10^{-9}$ Gauss and we get

$$k_{\rm max} \gtrsim \frac{1}{l_g} \left(\frac{2\pi/25{\rm kpc}}{k_B} \right)^{\frac{2}{3}} \,, \tag{44}$$

which is more restrictive then eq. (37). As n increases, the constraint becomes less severe, since the steeper the spectrum the less it contributes to $\bar{B}_l$.

We now return to the ranges in $k_{\rm max}$ and k_B which are relevant for structure formation. In an analogous way to the delta function case, small scales grow faster than larger scales, and the first scales to become non-linear have $k \sim \min(2k_{\rm max}, k_B)$. We again define $t_{nl}(k)$, such that $\Delta_n(k, t_{nl}) = 1$. For $2k_{\rm max} > k_B$, $\Delta_n(k_B, t_{nl}) = 1$ also leads to eq. (38) but with $\gamma_n \simeq 3.77 \times 10^{-2} (k_{\rm max}/k_B)^{3/2}/\epsilon_n$. The closer $k_{\rm max}$ is to $k_B/2$, the earlier structures on scales k_B can form.

Following the logic of the previous section, we find that for $k_{\rm max} \simeq k_B$, the first non-linear objects could form at redshift $z_{nl}(k_B) \simeq 300$ and today $k_{nl}(t_0) \simeq 0.15\ k_B$. Again, if we set $k_{nl}(t_0) = 2\pi/8$ Mpc, then $k_{\rm max} \simeq k_B \simeq 2\pi/1$ Mpc, which satisfies eq. (26) but does not satisfy eq. (44). Although perturbations on scales k_B grow faster than in the previous case, the constraint from the galactic field is more severe. If instead, we choose $k_{nl}(t_0) = 2\pi/2$ Mpc, for example, then $k_{\rm max} \simeq k_B \simeq 2\pi/0.3$ Mpc which satisfies eq. (44) with $\langle B_0^2 \rangle^{1/2} \simeq 10^{-8}$ Gauss and $\bar{B}(l_g, t_0) \simeq 10^{-10}$ Gauss.

The time at which modes with $k = k_B$ become non-linear, $t_{nl}(k_B)$, increases as $k_{\rm max}/k_B$ grows from unity. For magnetic fields to play a role in structure formation, $t_{nl}(k_B)$ must be less than the age of the universe, t_0, which implies that $k_{\rm max} \lesssim 6k_B$.

As $k_{\rm max}/k_B$ decreases, so does $t_{nl}(k_B)$ up to $k_{\rm max} = k_B/2$, where the cutoff changes from k_B to $2k_{\rm max}$. For $2k_{\rm max} < k_B$, in order to find when the first objects form, we follow $t_{nl}(k)$ using our solution in the limit $k \ll k_B$ ($m \simeq 5$) which implies:

$$\left(\frac{t_{nl}(k)}{t_{\rm rec}}\right)^{\frac{2}{3}} \simeq \frac{1.5}{\epsilon_n}\left(\frac{k_{\rm max}}{k_B}\right)^{\frac{3}{2}}\left(\frac{k_B}{k}\right)^{\frac{7}{2}} . \tag{45}$$

From eq. (45), requiring $t_{nl}(k \simeq 2k_{\rm max}) \lesssim t_0$ leads to the constraint $k_{\rm max} \gtrsim 10^{-2}k_B$. This is an approximate estimate for the lower limit for $k_{\rm max}$, since eq. (45) was derived in the limit of $k \ll k_{\rm max}$. This estimate helps define the range for which magnetic fields can make non-linear structures, i.e., $10^{-2}k_B \lesssim k_{\rm max} \lesssim 6k_B$. For example, we can choose $k_{\rm max} \simeq 0.1k_B$, which gives $z_{nl}(k_{\rm max}) \simeq 7$. Choosing $k_{\rm max} \simeq 2\pi/0.8$ Mpc, then $k_B \simeq 2\pi/80$ kpc and all the observational constraints are satisfied, with $\langle B_0^2\rangle^{1/2} \simeq 3 \times 10^{-9}$ Gauss and $\bar{B}(l_g, t_0) \simeq 10^{-10}$ Gauss. On the other hand, if $k_{\rm max} \simeq 10^{-2}k_B \simeq 2\pi/8$ Mpc, then $t_{nl}(2k_{\rm max}) \simeq t_0$ and $k_B = 2\pi/0.08$ Mpc which satisfies eq. (26) but violates eq. (44).

We see that with a more realistic choice of power spectrum for magnetic fields at recombination, non-linear structures in the cosmologically relevant range of scales can be formed at reasonable redshifts for observationally viable field strengths. We concentrated on galaxy scales in our examples above, but another possible consequence of magnetic fields at recombination is the formation of smaller objects, such as QSO's or Pop III stars, at very early times. The scales on which magnetic fields generate structure are primarily in the non-linear regime, which limits our ability to make precise predictions within linear perturbation theory. In the case of the baryonic universe studied above, the range of scales affected by magnetic fields is quite narrow, which suggests that objects formed via magnetic field perturbations may be biased with respect to large scale structures formed by primordial perturbations.

4. Incompressible mode

We now turn to the incompressible or transverse modes, which are also solutions of eqs. (6)–(11). First, note that the incompressible modes do not affect the compressible modes just studied, and vice-versa, an assertion which can be demonstrated by considering eq. (20) in detail.

In order to study the incompressible modes, we take the curl and the time derivative of eq. (6), use eqs. (7)–(12), and find

$$\nabla \times \left(\partial_{tt} \mathbf{v} + \frac{2}{t} \partial_t \mathbf{v} + \frac{2}{9t^2} \mathbf{v} \right) = \left(\frac{t_o}{t} \right)^2 \frac{\nabla \times \mathbf{Q}}{4\pi \rho_0}, \tag{46}$$

which is the imcompressible analog of eq. (15). We then take Fourier transforms as in eqs. (16)–(17), and obtain the analog of eq. (22) for the incompressible mode:

$$\left\{ \partial_{TTT} + 3\partial_{TT} + \left(\frac{26}{9} + \frac{2}{3} ak^2 \right) \partial_T + \left(\frac{2}{3} ak^2 + \frac{8}{9} \right) \right\} \langle |\tilde{v}_\perp(\mathbf{k}, t)|^2 \rangle = 0, \tag{47}$$

where $k\dot{\tilde{v}}_\perp(\mathbf{k}, t_{\rm rec}) \equiv |\mathbf{k} \times \dot{\tilde{\mathbf{v}}}(\mathbf{k}, t_{\rm rec})|$.

Since the calculation is essentially the same as that described above for the compressible case, we only present the solution for the incompressible case here:

(i) for $ak^2 \neq 1/6$:

$$\tilde{v}_{\perp,\rm rms}(k,t) = \dot{\tilde{v}}_{\perp,\rm rms}(k, t_{\rm rec}) \frac{t_{\rm rec}}{2p} \left(\frac{t}{t_{\rm rec}} \right)^{-\frac{1}{2}} \left[\left(\frac{t}{t_{\rm rec}} \right)^p - \left(\frac{t}{t_{\rm rec}} \right)^{-p} \right], \tag{48a}$$

(ii) for $ak^2 = 1/6$:

$$\tilde{v}_{\perp,\rm rms}(k,t) = \dot{\tilde{v}}_{\perp,\rm rms}(k, t_{\rm rec}) t_{\rm rec} \left(\frac{t}{t_{\rm rec}} \right)^{-\frac{1}{2}} \ln \left(\frac{t}{t_{\rm rec}} \right), \tag{48b}$$

where $\tilde{v}_{\perp,\rm rms}(k,t) \equiv \sqrt{\langle |\tilde{v}_\perp(\mathbf{k}, t)|^2 \rangle}$, $p(k) \equiv \sqrt{1 - 6ak^2}/6$. and $a = \langle B_0^2 \rangle / 12\pi^2 \rho_0^2 G$ is the same as in the compressible case. Unlike the compressible modes, the incompressible modes have no growing solution, only decaying or damped oscillatory solutions.

The initial value of $\dot{\tilde{v}}_{\perp,\rm rms}(k, t_{\rm rec})$ can be obtained from eq. (6) by taking the curl,

$$\nabla \times \dot{\mathbf{v}}(\mathbf{x}, t_{\rm rec}) = \frac{\nabla \times [(\nabla \times \mathbf{B}_0) \times \mathbf{B}_0]}{4\pi \rho_0 R_{\rm rec}^2}. \tag{49}$$

Again, as in the compressible case $\langle \dot{\tilde{v}}_\perp(\mathbf{k}, t_{\rm rec}) \rangle = 0$.

If we assume a power law Ansatz for the magnetic field spectrum, as in eq. (40), we find for the imcompressible velocity field spectrum:

$$\dot{\tilde{v}}_{\perp,\rm rms}(k, t_{\rm rec}) \simeq \frac{(n+3) \langle B_0^2 \rangle k}{(4\pi)^3 \rho_0 R_{\rm rec}^2} \sqrt{\frac{28V}{15(2n+3) k_{\rm max}^3}}. \tag{50}$$

Comparing to eq. (41), we see that the incompressible mode is initially excited to almost the same extent as the compressible mode. Although the two modes have comparable "initial" amplitude and spectrum, they have quite different time evolution, and do not mix with each other as time evolves.

5. Conclusions

We have studied the effects of magnetic fields present at recombination on the origin and evolution of density perturbations and the peculiar velocity field. We find there are generic features of the generated density perturbations which are largely independent of the assumed spectrum of the primordial magnetic field. The first conclusion we can draw is that magnetic fields cannot explain the observed galaxy power spectrum on large scales, since the generated spectrum $P(k) \propto k^4$ for small k.

Another generic feature is the cutoff introduced by the magnetic Jeans length. This cutoff limits the amplitude of the power spectrum for any choice of magnetic field strength. As the magnetic field strength increases, the amplitude for a given density perturbation mode rises, but, simultaneously, the magnetic Jeans cutoff moves to smaller k. The net effect, in the case of power law magnetic field spectra, is that the peak amplitude for the density power spectrum is independent of $\langle B_0^2 \rangle$.

Since the generated spectrum falls sharply at small k and is cut off at large k, magnetic fields generally produce a peak in the density spectrum over a narrow range of wavenumbers. For this peak to be of relevance to the formation of structure, the amplitude $\Delta(k, t_0)$ must be $\gtrsim 1$ for scales $k^{-1} \lesssim 8$ Mpc. The peak amplitude is sensitive to the assumed spectrum for the primordial magnetic field; the smaller $k_{\rm max}$, the stronger the variance in the density perturbations. In particular, if $k_{\rm max} \lesssim k_B$, density variances well above unity can be obtained with relatively small magnetic fields. Depending on k_B and $k_{\rm max}$, objects from galaxy scales down to a first generation of massive stars can be formed. As the variance reaches unity our calculations break down, and another conclusion can be drawn: when magnetic fields are important, their effects are mostly non-linear in nature. Our linear calculations can, however, be used to estimate the epoch of non-linear collapse of different mass scales.

In the present work, we have focused on a purely baryonic universe. In a subsequent paper, we study the evolution of density perturbations when non-baryonic dark matter is the dominant component of the universe. When we include non-relativistic (cold) dark matter, we find that the amplitude of the density perturbations decreases as Ω_B decreases for a fixed magnetic field strength. On the other hand, the perturbations become unstable for all wavenumbers: since cold dark matter does not couple to the magnetic fields, no oscillatory modes can be sustained. In this case, the perturbation amplitude $\Delta(k)$ flattens out for large k rather than being cutoff at k_B. Baryons will still show some resistance to clumping on small scales due to the magnetic field; this may segregate baryons from dark matter, introducing a source of bias on small scales.

In the case of hot dark matter the growth of baryon perturbations on small scales is slower due to neutrino free-streaming. Therefore, the initial perturbations need to be much larger for the final variance to be greater than 1. Clearly, the hot dark matter scenario would greatly benefit from a peak in the variance at large k so that structures can form on scales smaller than the neutrino free-streaming length and populate the problematic empty voids.

Finally, we conclude by noting that magnetic fields most likely play a dynamical role in the formation of galaxies and clusters of galaxies even if the original perturbations were caused by other sources.

Acknowledgements:

We thank J. Frieman, A. Stebbins, S.I. Vainshtein, and I. Wasserman for useful discussions. This work was supported in part by a NASA Astrophysics Theory grant to the Univ. of Chicago and NASA grant NAG 5-2788 at Fermilab.

Figure Captions

Fig. 1: The transfer function $\tau(k,t)$ plotted versus k/k_B for redshifts $z = 0, 1, 5, 10, 100$, and 1000. (We chose $k_{\rm rec} = 0.01 k_B$.)

Fig. 2: The variance for the delta function Ansatz Δ_δ in units of k_B/k_* as a function of k/k_B for redshifts $z = 0, 1, 5, 10, 100$, and 1000. (We chose $k_{\rm rec} = 0.01 k_B$.)

Fig. 3: The variance for the power law Ansatz Δ_n in units of $\epsilon_n (k_B/k_{\rm max})^{\frac{3}{2}}$ as a function of k/k_B for redshifts $z = 0, 1, 5, 10, 100$, and 1000. (We chose $k_{\rm rec} = 0.01 k_B$.)

REFERENCES

Barrow, J. 1976, MNRAS, 175, 359

Chandrasekhar, S., & Fermi, E. 1953, ApJ, 118, 116

Cheng, B., & Olinto, A.V. 1994, Phys. Rev. D, 50, 2421

Coles, P. 1992, Comments Astrophys., 16, 45

Collins, C.A., Nichol, R.C., & Lumsden, S. L. 1992, MNRAS, 254, 295

Efstathiou, G., et al. 1990, MNRAS, 247, 10P

Fisher. K. B., et al. 1993, ApJ, 402, 42

Ganga, K., Cheng, E., Meyer, S., & Page, L. 1993, ApJ (Letters), 410, L57

Geller. M., & Huchra, J. 1989, Science, 246, 897

Hogan. C.J. 1983, PRL, 51, 1488

Kolb, M.W., & Turner, M.S. 1990, *The Early Universe* (Redwood City: Addision–Wesley Publishing Company)

Kraichnan, R.H., & Nagarajan, S. 1967, Phys. Fluids, 10, 859

Kronberg, P.P. 1994, *Rep. Prog. Phys.*, in press

Maddox, S.J., et al. 1990, MNRAS, 246, 433

Moffatt, H.K. 1978, *Magnetic Field Generation in Electrically-Conducting Fluids* (Cambridge: Cambridge Univ. Press).

Peebles, P.J.E. 1980, *The Large–Scale Structure of The Universe* (Princeton: Princeton Univ. Press)

Peebles, P.J.E. 1993, *Principles of Physical Cosmology* (Princeton: Princeton University Press)

Quashnock, J., Loeb, A., & Spergel, D.N. 1989, ApJ (Letters), 344, L49

Ratra, B. 1993, ApJ (Letters), 391, L1

Smoot, G., et al. 1992, ApJ (Letters), 396, L1

Turner, M.S., & Widrow, L.M. 1988, Phys. Rev. D, 30, 2743

Vainshtein, S.I., & Zeldovich, Ya.B. 1972, Sov. Phys. Uspekhi, 15, 159

Vaschaspati, T. 1991, Phys. Lett. B, 265, 258

Walker, T., et al. 1991, ApJ, 376, 51

Wasserman, I. 1978, ApJ, 224, 337

Wolfe, A.M. 1988 in *QSO Absorption Lines: Probing the Universe*, ed. Blades, C.J., et al. (Cambridge: Cambridge Univ. Press), 297

Wolfe, A.M., Lanzetta. K.M., & Oren, A.L. 1991, ApJ, 388, 17

Appendix A

In this Appendix, we demonstrate that $\langle B_{\rm rec}\tilde{v}_{\parallel}(t)\rangle = \langle B_{\rm rec}\tilde{v}_{\perp}(t)\rangle = 0$. We begin with the evolution equation for $\tilde{v}_{\parallel}$, obtained simply by taking the inner product of eq. (19) with $\mathbf{k}$, so that

$$k\left(t^2\partial_{tt} + 2t\partial_t - \frac{4}{9}\right)\tilde{v}_{\parallel}(\mathbf{k},t) = \beta\int d^3\mathbf{k}_1 d^3\mathbf{k}_2\ F(\mathbf{k},\mathbf{k}_1,\mathbf{k}_2,\tilde{\mathbf{B}}(\mathbf{k}_1),\tilde{\mathbf{B}}(\mathbf{k}_2),\tilde{\mathbf{v}}(\mathbf{k}-\mathbf{k}_1-\mathbf{k}_2,t)) \qquad (A1)$$

With the use of the Green function for this equation,

$$G(t,t') = \frac{3\theta(t-t')}{5kt'}\left[\left(\frac{t'}{t}\right)^{-\frac{1}{3}} - \left(\frac{t'}{t}\right)^{\frac{4}{3}}\right]. \qquad (A2)$$

(where θ is the step function), one can solve eq. (A1) formally, given the initial conditions

$$\tilde{v}_{\parallel}(k,t_{\rm rec}) = 0$$

and

$$\partial_t\tilde{v}_{\parallel}(k,t)|_{t=t_{\rm rec}} = \dot{\tilde{v}}_{\parallel}(k,t_{\rm rec})\,.$$

This Green's function solution is given by

$$\tilde{v}_{\parallel}(k,t) = \frac{3t_{\rm rec}\dot{\tilde{v}}_{\parallel}(k,t_{\rm rec})}{5}\left[\left(\frac{t_{\rm rec}}{t}\right)^{-\frac{1}{3}} - \left(\frac{t_{\rm rec}}{t}\right)^{\frac{4}{3}}\right] + \beta\int_{t_{\rm rec}}^{t} dt'\int d^3\mathbf{k}_1 d^3\mathbf{k}_2 G(t,t')F(\mathbf{k},\mathbf{k}_1,\mathbf{k}_2,\tilde{\mathbf{B}}(\mathbf{k}_1),\tilde{\mathbf{B}}(\mathbf{k}_2),\tilde{\mathbf{v}}(\mathbf{k}-\mathbf{k}_1-\mathbf{k}_2,\mathbf{t}'))(A3)$$

This equation can be solved by iteration, yielding a Born-series-like solution, for which the zeroth-order iterate $\tilde{v}_{\parallel}^0(k,t)$ is given by

$$\tilde{v}_{\parallel}^0(k,t) = \frac{3t_{\rm rec}\dot{\tilde{v}}_{\parallel}(k,t_{\rm rec})}{5}\left[\left(\frac{t_{\rm rec}}{t}\right)^{-\frac{1}{3}} - \left(\frac{t_{\rm rec}}{t}\right)^{\frac{4}{3}}\right]. \qquad (A4)$$

We first note that $\langle\tilde{v}_{\parallel}^0(k,t)B_{\rm rec}\rangle = 0$. This result is obtained simply by noting that $\dot{\tilde{v}}_{\parallel}^0(k,t_{\rm rec})$ is quadratic in $B_{\rm rec}$ (cf. eq. (20)), so that $\tilde{v}_{\parallel}^0(k,t)B_{\rm rec}$ is an odd product of $B_{\rm rec}$. Hence, as long as $B_{\rm rec}$ is a random variable governed by Gaussian statistics, $\langle\tilde{v}_{\parallel}^0(k,t)B_{\rm rec}\rangle$ must vanish since all odd moments of a Gaussian random variable vanish.

It is now straightforward to demonstrate that $\langle \tilde{v}_{\parallel}(k,t)B_{\rm rec}\rangle = 0$ to all orders by simply computing the next-order iterates: At the $n^{\rm th}$ iteration stage, $\tilde{v}_{\parallel}^{n}(k,t)$ is the sum of even products of $B_{\rm rec}$ (because F is a quadratic form in $B_{\rm rec}$); hence, $\tilde{v}_{\parallel}^{n}(k,t)B_{\rm rec}$ must be always an odd product of $B_{\rm rec}$, and therefore $\langle \tilde{v}_{\parallel}^{n}(k,t)B_{\rm rec}\rangle = 0$, as before. Thus, under the assumption that the Born series expansion converges, we obtain a portion of our desired result, namely that

$$\langle \tilde{v}_{\parallel}(k,t)B_{\rm rec}\rangle = 0\,.$$

It is now readily shown that the same result obtains for the incompressible flow, $\tilde{v}_{\perp}$, by simply repeating the above calculation, but now projecting out the incompressible component. Thus, we also obtain $\langle \tilde{v}_{\perp}(k,t)B_{\rm rec}\rangle = 0$, and hence we have the ultimately desired result that

$$\langle \tilde{v}(k,t)B_{\rm rec}\rangle = 0\,.$$

Appendix B

In this Appendix, we show how to obtain $\tilde{\delta}_{\rm rms}(k,t)$ from $\tilde{v}_{\rm rms}(k,t)$. We start with eq. (20) in the main text, which reads

$$(\partial_{TT} + \partial_T - \frac{4}{9})\tilde{v}_{\parallel}(\mathbf{k},T) = \frac{\beta}{k}G_i(\mathbf{k}:\mathbf{l})v_i(\mathbf{l},T)\,. \tag{B1}$$

Upon using $T \equiv \ln t$, this is equivalent to

$$(t^2\partial_{tt} + 2t\partial_t - \frac{4}{9})\tilde{v}_{\parallel}(\mathbf{k},t) = \frac{\beta}{k}G_i(\mathbf{k}:\mathbf{l})v_i(\mathbf{l},t)\,. \tag{B2}$$

The *rms* solution to (B2) was shown to be given by eq. (23) in the main text, which we rewrite as

$$\tilde{v}_{\parallel,\rm rms}(k,t) = \dot{v}_{\parallel,\rm rms}(k,t_{\rm rec})V(t)\ , \tag{B3}$$

where

$$V(t) \equiv \frac{3t_{\rm rec}}{m}\left(\frac{t}{t_{\rm rec}}\right)^{-\frac{1}{6}}\left[\left(\frac{t}{t_{\rm rec}}\right)^{\frac{m}{6}} - \left(\frac{t}{t_{\rm rec}}\right)^{-\frac{m}{6}}\right],$$

$\tilde{v}_{\rm rms}(k,t) \equiv \sqrt{<|\tilde{v}_{\parallel}(\mathbf{k},t)|^2>}$, and $m \equiv \sqrt{25 - 12ak^2}$.

First, multiply both sides of eq. (B2) by $\tilde{v}_{\parallel}^{*}(\mathbf{k},t')$, with $t' \neq t$, and then take an average to get the following equation:

$$(t^2\partial_{tt} + 2t\partial_t - \frac{4}{9})\langle\tilde{v}_{\parallel}(\mathbf{k},t)\tilde{v}^*_{\parallel}(\mathbf{k},t')\rangle = \frac{\beta}{k}\langle G_i(\mathbf{k}:\mathbf{l})v_i(\mathbf{l},t)\tilde{v}^*_{\parallel}(\mathbf{k},t')\rangle\,. \qquad (B4)$$

Now after repeating the same calculation that was used to get eq. (22) from eq. (21), it can be shown that

$$\langle G_i(\mathbf{k}:\mathbf{l})\tilde{v}_i(\mathbf{l},t)\tilde{v}^*_{\parallel}(\mathbf{k},t')\rangle = -\frac{2}{3}\langle B_0^2\rangle k^3\langle\tilde{v}_{\parallel}(\mathbf{k},t)\tilde{v}^*_{\parallel}(\mathbf{k},t')\rangle\,. \qquad (B5)$$

Using eq. (B5), we readily obtain the solution to eq. (B4), namely

$$\langle\tilde{v}_{\parallel}(\mathbf{k},t)\tilde{v}^*_{\parallel}(\mathbf{k},t')\rangle = \langle\dot{\tilde{v}}_{\parallel}(\mathbf{k},t_{\rm rec})\tilde{v}^*_{\parallel}(\mathbf{k},t')\rangle V(t)\,. \qquad (B6)$$

Next, let us take complex conjugate of both sides of eq. (B2), multiply by $\dot{\tilde{v}}_{\parallel}(\mathbf{k},t_{\rm rec})$, and then take an average; that gives

$$\langle\tilde{v}^*_{\parallel}(\mathbf{k},t)\dot{\tilde{v}}_{\parallel}(\mathbf{k},t_{\rm rec})\rangle = \langle|\dot{\tilde{v}}_{\parallel}(\mathbf{k},t_{\rm rec})|^2\rangle V(t)\,. \qquad (B7)$$

From eqs. (B3) and (B7),

$$\langle\tilde{v}^*_{\parallel}(\mathbf{k},t)\dot{\tilde{v}}_{\parallel}(\mathbf{k},t_{\rm rec})\rangle = \sqrt{\langle|\dot{\tilde{v}}_{\parallel}(\mathbf{k},t_{\rm rec})|^2\rangle}\sqrt{\langle|\tilde{v}_{\parallel}(\mathbf{k},t)|^2\rangle}\,,$$

or

$$\langle\tilde{v}^*_{\parallel}(\mathbf{k},t')\dot{\tilde{v}}_{\parallel}(\mathbf{k},t_{\rm rec})\rangle = \sqrt{\langle|\dot{\tilde{v}}_{\parallel}(\mathbf{k},t_{\rm rec})|^2\rangle}\sqrt{\langle|\tilde{v}_{\parallel}(\mathbf{k},t')|^2\rangle}\,. \qquad (B8)$$

Upon using eq. (B8) in eq. (B6)

$$\langle\tilde{v}_{\parallel}(\mathbf{k},t)\tilde{v}^*_{\parallel}(\mathbf{k},t')\rangle = \sqrt{\langle|\dot{\tilde{v}}_{\parallel}(\mathbf{k},t_{\rm rec})|^2\rangle}\sqrt{\langle|\tilde{v}_{\parallel}(\mathbf{k},t')|^2\rangle}V(t)\,. \qquad (B9)$$

Finally, with the help of eq. (B3), eq. (B9) becomes

$$\langle\tilde{v}_{\parallel}(\mathbf{k},t)\tilde{v}^*_{\parallel}(\mathbf{k},t')\rangle = \sqrt{\langle|\tilde{v}_{\parallel}(\mathbf{k},t)|^2\rangle}\sqrt{\langle|\tilde{v}_{\parallel}(\mathbf{k},t')|^2\rangle}\,. \qquad (B10)$$

On the other hand, eq. (7) in the main text gives us the following equation:

$$ik\frac{\tilde{v}_{\parallel}(\mathbf{k},t)}{R(t)} = -\frac{\partial}{\partial t}\tilde{\delta}(\mathbf{k},t)\,. \qquad (B11)$$

By integrating eq. (B11), the solution for the density fluctuations is

$$\tilde{\delta}(\mathbf{k},t) = -ik \int_{t_{rec}}^{t} dt' \, \frac{\tilde{v}_{\parallel}(\mathbf{k},t')}{R(t')} \,. \qquad (B12)$$

By multiplying by the complex conjugate of eq. (B12), and then taking its average, we obtain

$$\begin{aligned}
\langle|\tilde{\delta}(\mathbf{k},t)|^2\rangle &= k^2 \int_{t_{rec}}^{t} \frac{dt_1}{R(t_1)} \int_{t_{rec}}^{t} \frac{dt_2}{R(t_2)} \langle \tilde{v}_{\parallel}(\mathbf{k},t_1)\tilde{v}_{\parallel}^{*}(\mathbf{k},t_2)\rangle \\
&= k^2 \int_{t_{rec}}^{t} \frac{dt_1}{R(t_1)} \sqrt{\langle|\tilde{v}_{\parallel}(\mathbf{k},t_1)|^2\rangle} \int_{t_{rec}}^{t} \frac{dt_2}{R(t_2)} \sqrt{\langle|\tilde{v}_{\parallel}(\mathbf{k},t_2)|^2\rangle} \\
&= \left[k \int_{t_{rec}}^{t} \frac{dt_1}{R(t_1)} \sqrt{\langle|\tilde{v}_{\parallel}(\mathbf{k},t_1)|^2\rangle} \right]^2 , \qquad (B13)
\end{aligned}$$

where eq. (B10) has been used; taking the square root of eq. (B13), we obtain

$$\sqrt{\langle|\tilde{\delta}(\mathbf{k},t)|^2\rangle} = k \int_{t_{rec}}^{t} \frac{dt_1}{R(t_1)} \sqrt{\langle|\tilde{v}_{\parallel}(\mathbf{k},t_1)|^2\rangle} \,. \qquad (B14)$$

In other words,

$$\tilde{\delta}_{\mathrm{rms}}(k,t) = k \int_{t_{rec}}^{t} \frac{dt_1}{R(t_1)} \, \tilde{v}_{\mathrm{rms}}(k,t_1) \,. \qquad (B15)$$

The differential equation for $\tilde{\delta}_{\mathrm{rms}}$ follows via taking the time derivative of eq. (B15).

$$\frac{\partial}{\partial t} \tilde{\delta}_{\mathrm{rms}}(k,t) = k \frac{\tilde{v}_{\mathrm{rms}}(k,t)}{R(t)} \,. \qquad (B16)$$

Appendix C

In this Appendix, we show how to derive eqs. (31) and (41). We begin with eq. (29),

$$\nabla \cdot \dot{\mathbf{v}}(\mathbf{x},t_{\mathrm{rec}}) = \alpha \nabla \cdot [(\nabla \times \mathbf{B}_0) \times \mathbf{B}_0] \,, \qquad (C1)$$

where $\alpha \equiv 1/4\pi\rho_0 R_{\mathrm{rec}}^2$. By using the Fourier expressions in space for $\mathbf{v}$ and $\mathbf{B}_0$, we obtain

$$ik \cdot \dot{\mathbf{v}}(\mathbf{k}, t_{\rm rec}) = -\alpha \int d^3\mathbf{k}_1 \mathbf{k} \cdot \{\mathbf{B}(\mathbf{k}_1)[\mathbf{k}_1 \cdot \mathbf{B}(\mathbf{k}-\mathbf{k}_1)] - \mathbf{k}_1[\mathbf{B}(\mathbf{k}_1) \cdot \mathbf{B}(\mathbf{k}-\mathbf{k}_1)]\} \,, \quad (C2)$$

where $\mathbf{B} \equiv \tilde{\mathbf{B}}$ throughout this Appendix. If we choose our coordinate system in such a way that $\mathbf{k}$ is along z–axis,

$$\int d^3\mathbf{k}_1 = 4\pi \int dk_1 k_1^2 \int d\mu \,,$$

where $\mu \equiv \cos\theta$ with θ is the angle between the $\mathbf{k}_1$ and z–axis. The integration range in eq. (C2) should be taken carefully since the integrand had $\delta(\mathbf{k} - \mathbf{k}_1 - \mathbf{k}_2)$ before integrated over $\mathbf{k}_2$ with the condition of $k_{\rm min} \le k_i \le k_{\rm max}$ for $i = 1, 2$. In other words, there is a constraint on the angle to be integrated, depending on the magnitude of k_1. By taking into account this constraint, the integration range of eq. (C2) depends on the magnitude of k, and can be shown to be

(1) For $0 \le k \le k_{\rm min}$:

$$\int dk_1 d\mu = \int_{k_{\rm min}}^{k+k_{\rm min}} dk_1 \int_{-1}^{\frac{k^2+k_1^2-k_{\rm min}^2}{2kk_1}} d\mu + \int_{k+k_{\rm min}}^{k_{\rm max}-k} dk_1 \int_{-1}^{1} d\mu$$
$$+ \int_{k_{\rm max}-k}^{k_{\rm max}} dk_1 \int_{\frac{k^2+k_1^2-k_{\rm max}^2}{2kk_1}}^{1} d\mu \,. \quad (C3)$$

(2) For $k_{\rm min} < k < k_{\rm max}$:

$$\int dk_1 d\mu = \int_{k_{\rm min}}^{k-k_{\rm min}} dk_1 \int_{-1}^{1} d\mu + \int_{k-k_{\rm min}}^{k+k_{\rm min}} dk_1 \int_{-1}^{\frac{k^2+k_1^2-k_{\rm min}^2}{2kk_1}} d\mu$$
$$+ \int_{k+k_{\rm min}}^{k_{\rm max}-k} dk_1 \int_{-1}^{1} d\mu + \int_{k_{\rm max}-k}^{k_{\rm max}} dk_1 \int_{\frac{k^2+k_1^2-k_{\rm max}^2}{2kk_1}}^{1} d\mu \,. \quad (C4)$$

(3) For $k_{\rm max} \le k \le k_{\rm max} + k_{\rm min}$:

$$\int dk_1 d\mu = \int_{k_{\min}}^{k-k_{\min}} dk_1 \int_{\frac{k^2+k_1^2-k_{\max}^2}{2kk_1}}^{1} d\mu + \int_{k-k_{\min}}^{k_{\max}} dk_1 \int_{\frac{k^2+k_1^2-k_{\max}^2}{2kk_1}}^{\frac{k^2+k_1^2-k_{\min}^2}{2kk_1}} d\mu \ . \qquad (C5)$$

(4) For $k_{\max} + k_{\min} \leq k \leq 2k_{\max}$:

$$\int dk_1 d\mu = \int_{k_{\min}}^{k_{\max}} dk_1 \int_{\frac{k^2+k_1^2-k_{\max}^2}{2kk_1}}^{1} d\mu \ . \qquad (C6)$$

If we take the ensemble average of both sides of eq. (C2), and use eq. (18), we obtain

$$\langle \mathbf{k}\cdot\dot{\mathbf{v}}(\mathbf{k},t_{\rm rec})\rangle = 0 \, .$$

To calculate $\dot{v}_{\rm rms}(k,t_{\rm rec})$, we take the square of both sides of eq. (C2) and obtain

$$|\mathbf{k}\cdot\dot{\mathbf{v}}(\mathbf{k},t_{\rm rec})|^2 = \alpha^2 \int d^3\mathbf{k}_1 d^3\mathbf{k}_2 \{(-\mathbf{k}\cdot\mathbf{B}^*(\mathbf{k}_1))[\mathbf{k}_1\cdot\mathbf{B}^*(\mathbf{k}-\mathbf{k}_1)] + (\mathbf{k}\cdot\mathbf{k}_1)[\mathbf{B}^*(\mathbf{k}_1)\cdot\mathbf{B}^*(\mathbf{k}-\mathbf{k}_1)]\}$$
$$\times \{(-\mathbf{k}\cdot\mathbf{B}(\mathbf{k}_2))[\mathbf{k}_2\cdot\mathbf{B}(\mathbf{k}-\mathbf{k}_2)] + (\mathbf{k}\cdot\mathbf{k}_2)[\mathbf{B}(\mathbf{k}_2)\cdot\mathbf{B}(\mathbf{k}-\mathbf{k}_2)]\}, \qquad (C7)$$

We then take the ensemble average of both sides of eq. (C7), and express the fourth-order correlation of B as a sum of a product of second order correlations by assuming a Gaussian distribution for B. Since each fourth-order correlation gives three products of second-order ones, we obtain a total of twelve terms on the right hand side of eq. (C7). Applying eq. (18) to these twelve terms yields terms proportional to $\delta(\mathbf{k})$, $\delta(\mathbf{k}_1-\mathbf{k}_2)$ and $\delta(\mathbf{k}-\mathbf{k}_1-\mathbf{k}_2)$, respectively. Four of these terms (which contain $\delta(\mathbf{k})$) vanish upon integration, so that they will not be written here; retaining the remaining eight terms leads to the expression

$$\begin{aligned}
\langle|\mathbf{k}\cdot\dot{\mathbf{v}}(\mathbf{k},t_{\rm rec})|^2\rangle = \alpha^2 \int d^3\mathbf{k}_1 d^3\mathbf{k}_2 \{ & \langle(\mathbf{k}\cdot\mathbf{B}^*(\mathbf{k}_1)\mathbf{k}\cdot\mathbf{B}(\mathbf{k}_2)\rangle\langle\mathbf{k}_1\cdot\mathbf{B}^*(\mathbf{k}-\mathbf{k}_1)\mathbf{k}_2\cdot\mathbf{B}(\mathbf{k}-\mathbf{k}_2)\rangle \\
& + (\mathbf{k}\cdot\mathbf{k}_1)(\mathbf{k}\cdot\mathbf{k}_2)\langle B_i^*(\mathbf{k}_1)B_j(\mathbf{k}_2)\rangle\langle B_i^*(\mathbf{k}-\mathbf{k}_1)B_j(\mathbf{k}-\mathbf{k}_2)\rangle \\
& - (\mathbf{k}\cdot\mathbf{k}_2)\langle\mathbf{k}\cdot\mathbf{B}^*(\mathbf{k}_1)B_i(\mathbf{k}_2)\rangle\langle\mathbf{k}_1\cdot\mathbf{B}^*(\mathbf{k}-\mathbf{k}_1)B_i(\mathbf{k}-\mathbf{k}_2)\rangle \\
& - (\mathbf{k}\cdot\mathbf{k}_1)\langle\mathbf{k}\cdot\mathbf{B}(\mathbf{k}_2)B_i^*(\mathbf{k}_1)\rangle\langle\mathbf{k}_2\cdot\mathbf{B}(\mathbf{k}-\mathbf{k}_2)B_i^*(\mathbf{k}-\mathbf{k}_1)\rangle \\
& + \langle(\mathbf{k}\cdot\mathbf{B}^*(\mathbf{k}_1)\mathbf{k}_2\cdot\mathbf{B}(\mathbf{k}-\mathbf{k}_2)\rangle\langle\mathbf{k}\cdot\mathbf{B}(\mathbf{k}_2)\mathbf{k}_1\cdot\mathbf{B}^*(\mathbf{k}-\mathbf{k}_1)\rangle \\
& + (\mathbf{k}\cdot\mathbf{k}_1)(\mathbf{k}\cdot\mathbf{k}_2)\langle B_i^*(\mathbf{k}_1)B_j(\mathbf{k}-\mathbf{k}_2)\rangle\langle B_i^*(\mathbf{k}-\mathbf{k}_1)B_j(\mathbf{k}_2)\rangle \\
& - (\mathbf{k}\cdot\mathbf{k}_2)\langle\mathbf{k}\cdot\mathbf{B}^*(\mathbf{k}_1)B_i(\mathbf{k}-\mathbf{k}_2)\rangle\langle\mathbf{k}_1\cdot\mathbf{B}^*(\mathbf{k}-\mathbf{k}_1)B_i(\mathbf{k}_2)\rangle \\
& - (\mathbf{k}\cdot\mathbf{k}_1)\langle\mathbf{k}\cdot\mathbf{B}(\mathbf{k}_2)B_i^*(\mathbf{k}-\mathbf{k}_1)\rangle\langle\mathbf{k}_2\cdot\mathbf{B}(\mathbf{k}-\mathbf{k}_2)B_i^*(\mathbf{k}_1)\rangle \} \\
\equiv \alpha^2 J. & \qquad (C8)
\end{aligned}$$

The integral of the these eight terms, J, is given by (using eq. (18)),

$$J = \frac{V}{(4\pi)^2}\int_{k_{\rm min}}^{k_{\rm max}} dk_1 \int_{-1}^{1} d\mu \frac{B^2(k_1)B^2(|\mathbf{k}-\mathbf{k}_1|)}{|\mathbf{k}-\mathbf{k}_1|^2}$$

$$\times\left\{2k^5k_1^3\mu + k^4k_1^4(1-5\mu^2) + 2k^3k_1^5\mu^3\right\}, \qquad (C9)$$

where the identity $\delta(\mathbf{k}=0) = V/(2\pi)^3$ has been used.

For the delta function Ansatz, $B^2(k) = A\delta(k-k_*)/4\pi k^2$, and therefore

$$J = \frac{VA^2}{(4\pi)^4}\frac{k^3}{k_*^2}, \qquad (C10)$$

where $A = \int d^3k\,\tilde{B}^2(k) \equiv \langle B_0^2\rangle$; eq. (31) follows from this result.

We now evaluate J for the case of a power law spectrum for $\tilde{B}^2(k)$, as in eq. (40). For simplicity, we assume $k_{\rm min} = 0$. The resulting integral can be solved analytically if we use $k/k_{\rm max}$ as a small parameter. In such an expansion, the leading order term turns out to be $(k/k_{\rm max})^3$ for $n=-2$, and $(k/k_{\rm max})^4$ for $n = -1$, 0, 1, 2, 3, 4, and 6. Finally, we find the following solution for the $n \geq -1$ case:

$$J = \frac{V}{(4\pi)^2}A^2k_{\rm max}^{2n+3}k^4\frac{22}{15(2n+3)}\left[1+O\left(\frac{k}{k_{\rm max}}\right)\right]. \qquad (C11)$$

So the total integral of eq. (C8) is

$$\langle|\mathbf{k}\cdot\dot{\mathbf{v}}(\mathbf{k},t_{\rm rec})|^2\rangle = k^2\dot{v}_{\parallel\rm rms}^2(\mathbf{k},t_{\rm rec}) \simeq \frac{\alpha^2V}{(4\pi)^4}A^2k_{\rm max}^{2n+3}k^4\frac{22}{15(2n+3)}, \qquad (C12)$$

where $\mathbf{k}\cdot\dot{\mathbf{v}}(\mathbf{k},t_{\rm rec}) = k\dot{v}_\parallel(\mathbf{k},t_{\rm rec})$ was used for the compressible mode. Finally, by applying $\langle B_0^2\rangle = \int_{k_{\rm min}}^{k_{\rm max}} d^3k\,Ak^n \simeq Ak_{\rm max}^{n+3}/(n+3)$ to the above equation (C12), we obtain eq. (41).

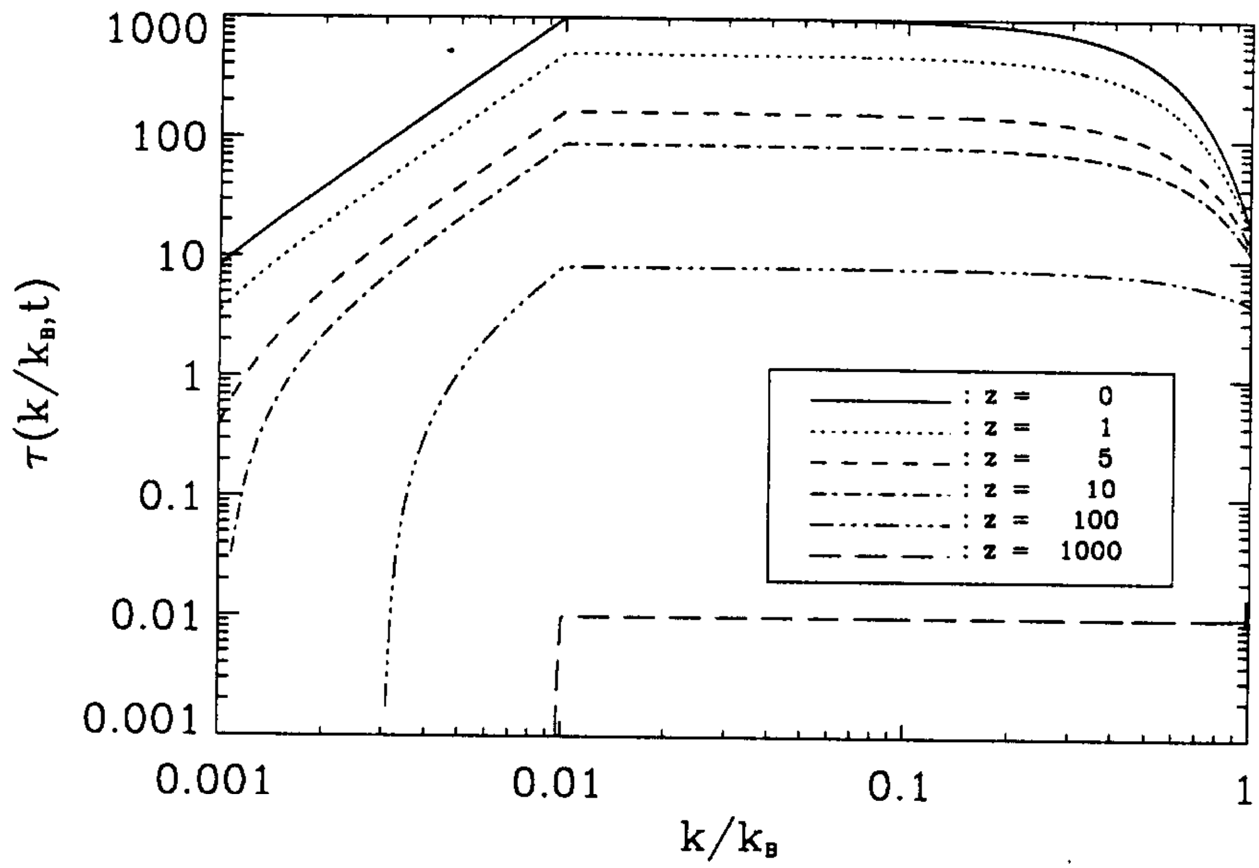
1000
100
10
1
0.1
0.01
0.001
0.001
0.01
0.1
1
$\tau(k/k_B,t)$
k/k_B
: z = 0
: z = 1
: z = 5
: z = 10
: z = 100
: z = 1000

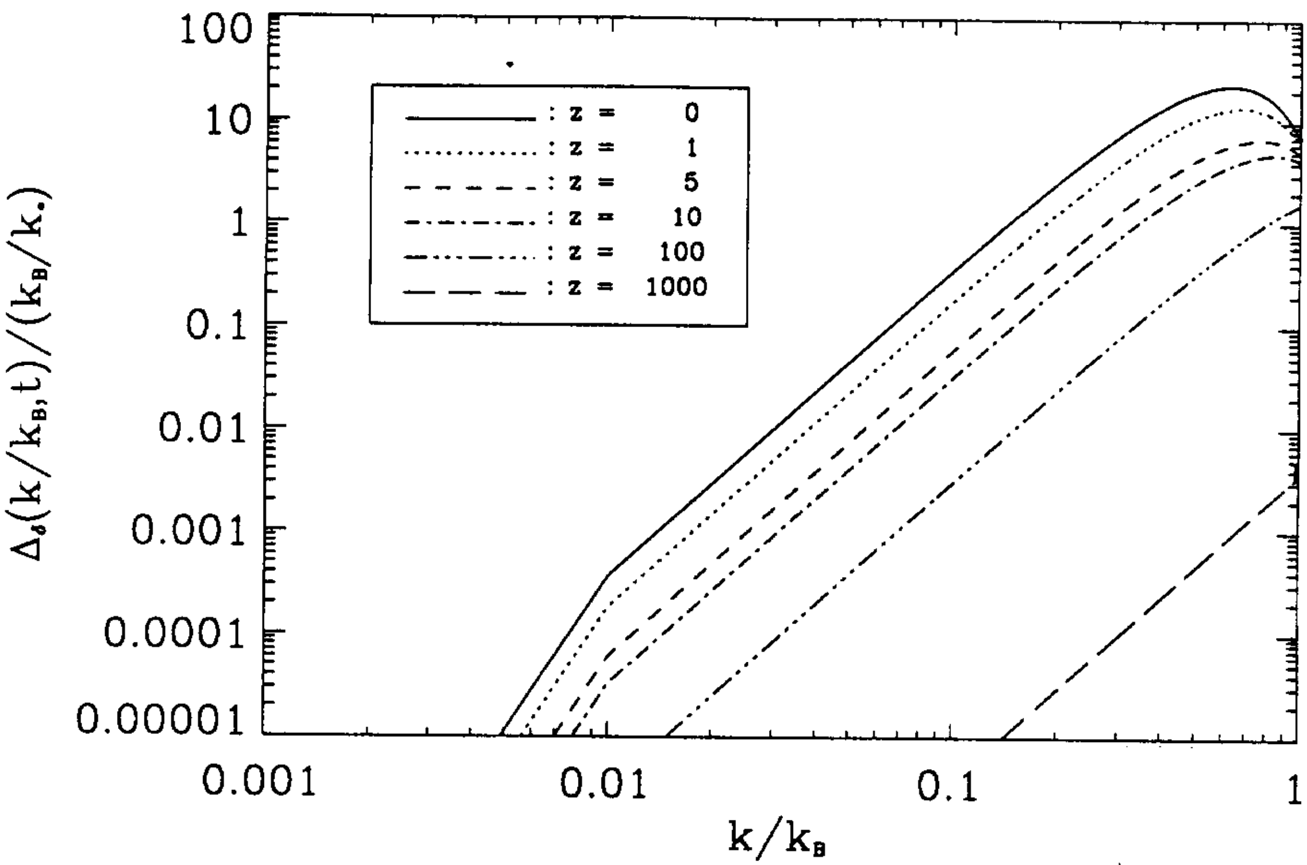

: z = 0
: z = 1
: z = 5
: z = 10
: z = 100
: z = 1000
100
10
1
0.1
0.01
0.001
0.0001
0.00001
0.001
0.01
0.1
1
Δ_δ(k/k_B,t)/(k_B/k_*)
k/k_B